The Serpentinite Multisystem Revisited: Chrysotile Is Metastable

Bernard W. Evans [a]

[a] University of Washington
Version of record first published: 14 Jul 2010.

PLEASE SCROLL DOWN FOR ARTICLE

The Serpentinite Multisystem Revisited: Chrysotile Is Metastable

BERNARD W. EVANS

Department of Earth and Space Sciences, University of Washington, Seattle, Washington 98195-1310

Abstract

The two rock-forming polymorphs of serpentine $Mg_3Si_2O_5(OH)_4$, lizardite and chrysotile, occur in nature in virtually identical ranges of temperature and pressure, from surficial or near-surficial environments to temperatures perhaps as high as 400°C. Laboratory evidence indicates that lizardite is the more stable at low temperatures, but the difference in their Gibbs free energies is not more than about 2 kJ in the 300–400°C range. Above about 300°C, antigorite + brucite is more stable than both; in other words, chrysotile is nowhere the most stable.

The crystal structures of lizardite and chrysotile give rise to contrasting crystallization behaviors and hence modes of occurrence. The hydration of peridotite at low temperature results in the growth of lizardite from olivine, and (commonly topotactically) from chain and sheet silicates, although the MgO-SiO_2-H_2O (MSH) phase diagram predicts antigorite + talc in bastite. The activity of H_2O during serpentinization may be buffered to low values by the solids, making the reaction of olivine to lizardite + brucite a stable one. Conservation of oxygen and inheritance of the Fe^{2+}/Mg exchange potential of olivine lead predictably to the precipitation of a highly magnesian lizardite and magnetite, and to the evolution of H_2. Volume expansion is made possible by lizardite's force of crystallization, and it is tentatively suggested that this might account for the α-serpentine orientation (length normal to (001)) of lizardite pseudofibers in mesh rims and hourglass pseudomorphs after olivine. Whereas mineral replacements commonly conserve volume, in massif serpentinites the diffusive loss of Mg and Si needed for volume conservation during serpentinization requires chemical potential gradients that are unlikely to exist. For small bodies of serpentinite, sheared serpentinite, and systems of large water/rock ratio, volume expansion may be much less.

Chrysotile is most conspicuously developed in tectonically active environments, where associated lithotypes show marginal greenschist-facies parageneses and antigorite tends to make its first appearance. Chrysotile growth is favored in isotropic stress microenvironments of fluid-filled voids and pores (where it may ultimately crystallize pervasively), and in veins, generally after active hydration in the immediate surroundings has ceased. This nevertheless allows the simultaneous growth of lizardite and chrysotile in adjacent partially and fully serpentinized peridotite, respectively, as in the cores and rims of kernel structures. Although prominent along shear surfaces, chrysotile growth as slip fiber is promoted by the presence of fluid rather than shear stress. Unlike lizardite, whose growth produces the stress associated with expansion, extreme flattening and shear might be expected to destroy the chrysotile structure. Thus, lizardite and chrysotile behave as though they were a stress-antistress mineral pair.

Calorimetric, solubility, and reaction-reversal experiments on chrysotile integrate contributions to its free energy arising from surface properties and, most importantly, from its radius-dependent strain energy. Minimally strained chrysotile (r ≈ 90 Å) may in fact be more stable than lizardite, whereas a maximal-radius chrysotile (r ≈ 200 Å) is not. A model for chrysotile in veins cutting lizardite- or antigorite-bearing rock involves nucleation of low-strain chrysotile followed by kinetically favored crystallization of higher-energy layers driven by mild fluid supersaturation maintained by local potential gradients. It is not clear if this explanation adequately accounts for serrate veins and mass-fiber chrysotile.

A revised phase diagram for lizardite and antigorite is offered, and possible stable and metastable reactions among the phases in serpentinites are followed on an isobaric diagram of reaction free energy (driving force) as a function of temperature. Composition-induced equilibrium shifts are believed unlikely to be determinative in most occurrences of Mg-rich lizardite and chrysotile. Circumstances of growth rather than temperature and pressure determine the occurrence of chrysotile vis-à-vis lizardite in serpentinites.

Introduction

IT IS A PLEASURE to present this paper in honor of Bob Coleman in recognition of his major, life-long contributions to the study of serpentinites, ophiolites, blueschists, and related tectonic issues. Bob introduced me to the New Idria serpentinite body on a field trip in 1964 or thereabouts, and engaged me in a collaborative study on brucite in alpine-type serpentinites (Hostetler et al., 1966). I have never lost interest in the things that this memorable introduction gave me.

The principal issue that this paper addresses is which of the one, two, or three common serpentine minerals—lizardite, chrysotile, and antigorite—correctly belongs in the phase diagram for the system MgO-SiO_2-H_2O (MSH) at crustal temperatures and pressures. In previous thermodynamic investigations of the serpentinite multisystem MSH (Evans et al., 1976; Helgeson et al., 1978; Trommsdorff, 1983; Day et al., 1985; Berman et al., 1986, Berman, 1988; Chernosky et al., 1988), only chrysotile and antigorite were considered for the phase diagram because the necessary experiments (high T-P phase equilibrium brackets, solubility measurements, calorimetry) had been done on these minerals but not on Al-free lizardite. Techniques for making the distinction between rock-forming chrysotile and lizardite *in situ* were not widely in use 30 years ago. A more recent PT diagram (O'Hanley and Wicks, 1995; O'Hanley, 1996, p. 160), based in part on oxygen-isotope thermometry of serpentine-magnetite pairs, shows a stable field for chrysotile between 195 and 260°C, with lizardite stable below and antigorite above. Their diagram recognizes that lizardite is volumetrically the most important serpentine mineral in serpentinites, especially retrograde-metamorphosed (hydrated) peridotites (Wicks and Whittaker, 1977; Wicks and Plant, 1979; O'Hanley et al., 1989), and reflects the views of many observers that a low-temperature stability field for lizardite is a strong possibility (e.g., Wicks and Plant, 1979; O'Hanley and Dyar, 1993; O'Hanley, 1996; Viti and Mellini, 1998). A question that has remained open until recently is whether lizardite owes its stability in natural serpentinites simply to dilution of the Mg component by the presence of R^{3+} cations such as Al, Cr, and Fe^{3+}.

By taking a hard look at all the relevant laboratory and field information, this paper attempts a critical assessment of the relative stabilities of chrysotile and lizardite in the system MSH. Recent

phase-equilibrium experiments of the bracketing kind have been few. On the other hand, investigations using characterization techniques with much more resolving power than polarized-light microscopy, notably microbeam XRD, SEM, TEM, and HRTEM, have revealed much new information regarding the occurrence of the various serpentine minerals in relation to their geologic environment, their microstructures, and the metamorphic processes involved in their formation. These investigations have provided us with a more refined understanding of the controls on the formation of serpentine minerals in nature.

Chrysotile and lizardite occur widely in serpentinites, commonly together, and correspond to inferred temperature conditions ranging from the surface up to perhaps as high as 400°C. A popular and entirely reasonable view is that both owe much of their growth in nature to kinetic factors that favor one or the other under different circumstances. This means that we must examine the contrasting processes by which chrysotile and lizardite form in nature. If the kinetic model is in fact the dominant influence, then of course the stable phase diagram loses much of its usefulness as a petrogenetic indicator, although the need still exists for basic reference-state thermodynamic data.

Kinetic Insights from Crystal Structures

The different crystal structures of the rock-forming Mg-serpentine minerals provide valuable clues to their crystallization mechanisms. The brief review of crystal structures that follows focuses on their crystallization behavior and its consequences. The structures of the serpentine minerals are based on 1:1 layers composed of a tetrahedral Si_2O_5 and an octahedral $Mg_3O_2(OH)_4$ sheet, and the different species result from the consequences of sheet attachment. A useful summary was provided by Wicks and O'Hanley (1988). In concentrating on terrestrial ultrabasic serpentinites and the system MSH, we should not forget the vast range in Fe/(Fe + Mg) ratios of serpentines in primitive carbonaceous chondrites (Brearley and Jones, 1997), whose study has relevance to the mineralogy of serpentines.

In *lizardite*, the layers are flat (Whittaker and Zussman, 1956), the geometric misfit of planar *t* and *o* sheets being accommodated principally by a coupled rotation of SiO_4 tetrahedra in the plane of the sheet, resulting in ditrigonal symmetry (Mellini, 1982; Mellini and Zanazzi, 1987; Mellini and Viti,

1994). This geometry promotes hydrogen bonding between the successive layers. The partial substitution of Al^{3+} and Fe^{3+} for Mg and Si also reduces misfit and stabilizes lizardite (Caruso and Chernosky, 1979). Lizardite $1T$ is by far the commonest polytype. Lizardite has been synthesized without great difficulty in the pure system MSH from olivine, oxide, and gel starting materials (Page, 1966; Iishi and Saito, 1973; Chernosky, 1975; Moody, 1976; Wegner and Ernst, 1983; Grauby et al., 1998).

According to O'Hanley (1991, 1996), the direct replacement of olivine in nature is to lizardite rather than to chrysotile. Nucleation of lizardite on the minerals of peridotite should be facilitated by the shared presence of planes of hexagonal close-packed oxygens. Cell dimensions indicate that the quality of two-dimensional (epitaxial; Bloss, 1994) concordance with lizardite declines in the order: sheet silicates > amphiboles > pyroxenes > olivine. Topotaxial (three-dimensional) replacement by lizardite is possible in the case of chlorite, and also in some chain silicates (e.g., Le Glueher et al., 1990). These considerations are relevant not only for nucleation and growth, but also in the context of possible stabilization (Bloss, 1994) of the product phase (lizardite or other planar serpentines).

In the case of olivine, Cressey (1979) found that the lizardite of mesh centers in contact with olivine is mostly randomly oriented, fine-grained, and strained. Viti and Mellini (1998) argued that the olivine-to-lizardite reaction is not topotactic because, in mesh-textured pseudomorphs, the lizardite has analogous (radial) microtextural arrangements in three almost orthogonal directions. The curvature of lizardite "fibers" in hourglass texture points to the same conclusion. These observations are seemingly in contrast to evidence from the laboratory and field for the oriented transformation of serpentine to olivine (Dungan, 1977). In a flow-through hydration experiment (Normand et al., 2002), both epitaxially and randomly oriented growth of lizardite platelets on olivine was observed. An unanswered question at this time is whether possible initial oriented growth of lizardite on olivine might commonly be followed by its recrystallization. This could be related to a reorientation of (001) planes of lizardite so that they become normal to the local principal stress resulting from the expansion that accompanied hydration (see the section on field evidence below). Cressey (1979) argued that the well-oriented lizardite "fibers" of mesh rims represent the recrystallization of poorly crystallized serpentine. The ready epitaxial/topotax-

ial nucleation and growth of lizardite at the expense of pyroxenes, amphiboles, and sheet silicates in peridotite is obvious from the platy character of bastite pseudomorphs, which in most cases are composed predominantly of lizardite (Cressey and Zussman, 1976; Wicks and Whittaker, 1977; Cressey, 1979; Wicks and Plant, 1979; Veblen and Buseck, 1981; Wicks, 1986; Livi and Veblen, 1987). TEM study showed that topotaxy is good in pyroxene interiors, but not necessarily so at the edges (Le Glueher et al., 1990).

Lizardite forms platy or elongate crystals that in mesh-textured, pseudomorphic serpentinite are generally less than 2–3 microns in cross-section and characterized by the presence of stacking faults and polytypic disorder (Viti and Mellini, 1998; Dódony and Buseck, 2004). The fine grain size and poor crystallinity of rock-forming lizardite is presumably a function of its low temperature of crystallization, like clay minerals in general, and possibly also low water/rock ratios at the site of serpentinization. When present in veins, however, lizardite may be free from disorder and present as crystals as much as 2 millimeters long parallel to [001] (Viti and Mellini, 1997). Grain sizes smaller than a micron imply a significant surface energy (Kerrick, 1990). A very crude estimate of 650 J/mol for equant crystals of lizardite 0.5 micron across may be obtained by adopting a modest value of 0.5 J/m^2 for the surface energy of the hydrous phase (e.g., Majzlan et al., 2000). The combined effect of surface energy, polytypic variations, and crystal defects (dislocations, stacking disorder, bending) means that the molar Gibbs free energy of lizardite has a variability in nature of at least several hundreds of joules, independent of variation related simply to pressure, temperature, and composition.

Chrysotile partially overcomes t - o sheet misfit by adopting a curvature that effectively expands the t-sheet and contracts the o-sheet, at least in one direction along their surface of mutual contact, and this results in cylindrical, spiral, helical, and conical crystals (Yada, 1971, 1979; Yada and Iishi, 1974; Wicks and Whittaker, 1975). Several polytypes are known, the commonest being the two-layer $2M_{c1}$ structure. Chrysotile's curving-sheet structure has significant consequences, not the least of which is that it turns a sheet silicate into a fibrous mineral. Intralayer strain is minimal for a radius of curvature of about 88 Å (Whittaker, 1957). The increase in strain in layers of smaller and larger radii (Chisholm, 1992, Fig. 4; Baronnet and Devouard, 1996,

Fig. 4) limits the growth of chrysotile to cylinders with inner radii of ≈ 35 Å and outer radii of ≈ 150 Å (Yada, 1971), although in some instances as large as 400 Å (Mellini, 1986). Most of the volume of the chrysotile cylinder is contained in that part with radii greater than the strain minimum. Extended growth of chrysotile is therefore possible only parallel to the axis of curvature, which is the crystallographic *a*-axis in the $2M_{c1}$ polytype. Along with halloysite that also forms cylinders, chrysotile cannot be spatially homogeneous in its properties, and thus is not a phase in the Phase Rule sense. The properties of a mole of chrysotile will be a function of the range in radii over which the strain energy is integrated. We may expect the range present to be dependent on the conditions under which the chrysotile has grown; for example, greater supersaturation will favor larger radii (Baronnet and Devouard, 1996), whereas growth in smaller pores may tend to exclude the larger radii. Oriented growth of chrysotile on silicate substrates with conventional translational lattices is limited to one dimension (Yada and Iishi, 1974; Baronnet and Belluso, 2002), and the evidence from TEM studies of hollow cores and porous spaces between parallel fibrils, and growth in voids, shows clearly that chrysotile forms by a solution-crystallization rather than a largely solid-state mechanism. Porosity, and perhaps also the size and shape of the voids, appears to be a requirement for its growth.

Given their relative sizes, the surface energy of chrysotile fibrils is much greater than that of typical lizardite crystals. Again, for a possible surface energy of 0.5 J/cm^2, a 300 Å diameter chrysotile cylinder will have about 7 kJ/mol of surface energy. Although this estimate is very rough, it indicates that we are dealing in the case of chrysotile with significant amounts of surface energy. The two-dimensional constraint on crystal size means that, unlike lizardite and antigorite, grain coarsening over time can for chrysotile never lead to grain sizes that free the crystal from the burden of a substantial surface energy contribution to its molar free energy. The potential surface energy to be liberated by growing additional layers (fatter crystals) is not sufficient to compensate for the increase in strain energy present in further layers of progressively less curved chrysotile. Both energy terms, surface and strain, are included in the molar thermodynamic properties of bulk chrysotile in its standard state, whether determined by calorimetry (King et al., 1967), solubility (Hemley et al., 1977), or experimental reaction

reversal (e.g., Johannes, 1968; Chernosky, 1982). The magnitude and likely variability of the strain energy term of natural chrysotile and chrysotile formed from different starting materials (oxides vs. gels vs. olivine) may account for discrepancies found during optimization of the thermodynamic database (Helgeson et al., 1978; Berman, 1988).

Chrysotile has long been known to crystallize readily from oxide, gel, and olivine starting materials in the system MSH at elevated temperatures and pressures (e.g. Bowen and Tuttle, 1949; Noll, 1950; Yoder, 1952; Roy and Roy, 1954; Gillery, 1959; Pistorius, 1963; Johannes, 1968; Korytkova and Makarova, 1972; Iishi and Saito, 1973; Chernosky, 1975; Kalinin and Zubkov, 1981; Ueno et al., 1991; Grauby et al., 1998). Synthesis experiments provide large water/mineral ratios as well as high free-energy starting materials and corresponding degrees of supersaturation for the nucleation and growth of chrysotile. Normand et al. (2002) showed experimentally that chrysotile appears to require greater fluid supersaturation for growth from olivine as compared to lizardite. The two factors that appear to favor crystallization of chrysotile (presence of porosity and supersaturation) are open-system properties. However, the tight experimental bracketing of olivine-to-chrysotile reactions (Berman, 1988, Fig. 21) would appear to show that the necessary supersaturation is quite modest, and that, apparently in contrast to nature, chrysotile may form by hydration of olivine in the laboratory, provided that fluid is in excess. We cannot be surprised that the favored environment for chrysotile is in veins.

Whereas the 1:1 layers comprising lizardite and chrysotile are structurally very similar (as far as we know without full three-dimensional structure refinements of chrysotile), it is evident that the overall structures are sufficiently dissimilar to give rise to contrasting behaviors in nucleation and growth, and hence occurrence in nature. Variations in crystal quality and size, resulting from individual circumstances of growth, probably mean substantially overlapping Gibbs free energies, even under PT-conditions where there is an experimentally detectable difference in their stabilities when integrated over a large sample of both (see the section on laboratory evidence below).

Polygonal serpentine. Substantial growth of fibrils beyond the usual outer radius limits for chrysotile involves a loss of curvature and transition into planar structures. This is polygonal serpentine (Cressey and Zussman, 1976), previously known as

Povlen-type serpentine, a morphological term for "cylinders" that encompasses chrysotile (inside) and lizardite (outside). Cross-dimensions may reach as much as a micrometer. Polygonal serpentine when viewed end-on in TEM images is seen to be composed of 15 or 30 wedge-shaped sectors of planar serpentine (Cressey and Zussman, 1976; Cressey, 1979; Mellini, 1986; Yada and Wei, 1987; Mitchell and Putnis, 1988; Cressey and Whittaker, 1993; Baronnet et al., 1994; Viti and Mellini, 1997). In most cases the planar layers consist of special arrangements of lizardite polytypes (Banfield et al., 1995; Dódony and Buseck, 2004). Polygonal serpentine is not clearly defined by X-ray powder diffraction because crushing destroys the polygonal architecture (Mellini, 1986; Wicks, 2000); instead TEM examination is required. Non-fibrous splintery, "woody," massive, or platy "chrysotile" vein material identified by XRD (e.g., Post and Borer, 2000) almost always contains some polygonal serpentine. With growth of polygonal serpentine, the properties of chrysotile asbestos desired by industry (habit, size, flexibility) are gradually lost.

The existence in nature of polygonal serpentine is instructive. It means that there have been countless instances where the crystallization of chrysotile was followed by the growth of planar serpentine composed of polytypes of lizardite. Polygonal serpentine forms by recrystallization (polygonalization) of pre-existing chrysotile and by overgrowth and replacement of bundles of parallel, close-packed chrysotile fibrils (Cressey and Zussman, 1976; Mellini, 1986; Mitchell and Putnis, 1988; Grauby et al., 1998; Baronnet and Belluso, 2002). It is hard to believe that in all cases the change in identity of the serpentine was occasioned by some specific change in P, T, or fluid composition. It seems much more likely that, having reached its outer radius limit, additional growth of chrysotile is barred and further microstructural evolution must involve something new. The flatter curvature of the outer layer of chrysotile provides a substrate favorable for the attachment and growth of planar serpentine. Epitaxial growth of lizardite on chrysotile does not require a perfectly planar substrate; the gradation from planar to curved and roll structures in 7 Å serpentine has been reported in several TEM studies (Veblen and Buseck, 1979, 1981; Wicks, 1986; Wicks and O'Hanley, 1988). Whereas the polygonization of chrysotile (Baronnet and Belluso, 2002, Fig. 11) may be driven by the release of strain energy, this mechanism might be limited by the fact

that chrysotile of optimal curvature is only minimally strained. A phase transition is involved, so the process is similar to, but not quite the same as, the formation of polygonal arcs by the release of strain energy in microfolded layers of mica or chlorite in metamorphic rocks. Growth of polygonal serpentine beyond the outer edge of chrysotile is presumably driven by some combination of the energy lost in grain coarsening and in transition to a more stable phase.

Antigorite is composed of curved *t-o* layers that by inversion every 16 to 32 Å along the *a*-axis give rise to a wave-structure (Zussman, 1954; Kunze, 1961). It is one of many kinds of modulated layer-silicate structures (Guggenheim and Eggleton, 1988). Attachment across the plane of inversion involves the loss of variable amounts of $Mg(OH)_2$. A typical radius of curvature for each segment is 63 Å (Kunze, 1961). Unlike chrysotile, the degree of curvature is not a function of crystal size. Variability in super-lattice wavelength, measured by m, the number of tetrahedra along an entire wavelength, with m = 17 the most common value, gives antigorite a polysomatic character. It is compositionally related to the true serpentine polymorphs by a mass balance that for m = 17 corresponds to 17 serpentine minus 3 brucite, and an antigorite formula of $Mg_{48}Si_{34}O_{85}(OH)_{62}$. Specific wavelengths of the super-lattice and corresponding formulae are a function of growth temperature and pressure (Uehara and Shirozu, 1985; Mellini et al., 1987; Wunder et al., 2001) and maybe composition as well. Crystal defects are common, but they decrease in frequency with increasing metamorphic grade (Mellini et al., 1987; Auzende et al., 2002). Structural continuity between the antigorite and chrysotile forms of serpentine was observed by Veblen (1980).

Antigorite's modulated structure permits crystals made of minimally strained, corrugated *t-o* layers to grow in all three dimensions, with the result that natural antigorite occurs as flaky crystals that range in size up to more than a millimeter across, typically set in an interlocking, interpenetrating, or parallel schistose texture. The synthesis of antigorite has required generally higher temperatures and pressures than are needed to grow chrysotile and lizardite (Iishi and Saito, 1973), not because these higher values are required to enter the stability field of antigorite, but presumably because of the complex structure of antigorite. Its sluggish nucleation and growth kinetics relative to those of chrysotile,

lizardite, and forsterite (e.g., Martin and Fyfe, 1970; Wegner and Ernst, 1983) have permitted long-duration reversal experiments to be done on two chrysotile breakdown reactions (not involving antigorite) well into the stability field of antigorite (350 to 550°C, Berman, 1988, Fig. 21; Chernosky et al., 1988). Epitaxial relationships of antigorite with precursor chain and sheet silicates are seen in HRTEM images (e.g., Veblen, 1980), but Livi and Veblen (1987) found that interfaces parallel to the (001) planes of phlogopite show marked strain in the case of antigorite and only minor strain in the case of lizardite.

Other MSH minerals. The discovery of the asbestiform serpentine-group mineral carlosturanite (Compagnoni et al., 1985) gave us a fourth mechanism for relief of t–o misfit in this group, one involving a complex modulation of the t sheets. Compared to lizardite and chrysotile, carlosturanite, ideally $Mg_{21}[Si_{12}O_{28}(OH)_4](OH)_{30}.H_2O$, is poorer in Si and richer in OH, and also contains molecular H_2O (Mellini et al., 1985). Light brown fibers of carlosturanite have been found abundantly in veins with chrysotile and/or antigorite in numerous outcrops of fractured serpentinites in Italy (Belluso and Ferraris, 1991) and Sweden (Mellini and Zussman, 1986), and one can surely expect it to be found elsewhere. It is not known whether there might be circumstances where it could be more stable than the compositional equivalent: $6 Chr + 3 Brc + 3 H_2O$ at very low temperatures. TEM study (Mellini et al., 1985; Baronnet and Belluso, 2002) has shown that it can be replaced by chrysotile.

Balangeroite, with an ideal formula of $Mg_{42}O_6(OH)_{40}(Si_4O_{12})_4$ (Compagnoni et al., 1983), is much poorer than Chr in SiO_2 and poorer in H_2O than Chr + Brc (Bal + 14 H_2O = 8 Chr + 18 Brc). It is not a sheet silicate, hence not a serpentine mineral, although it occurs as brown fibers in serpentinite together with chrysotile, magnetite, and Fe-Ni alloys. Like carlosturanite, its stability is not known.

Stability and Occurrence of Antigorite

The low-temperature limit of stability of antigorite is relevant to the possible existence of stable PT fields for chrysotile and lizardite. Antigorite alone, according to the data of Berman (1988), is stable with respect to talc + chrysotile down to below 25°C. To the writer's knowledge, such very low grade antigorite has never been reported.

The upper limit of thermal stability of chrysotile and lizardite, assuming the typical, m = 17 composition of antigorite, is given by the H_2O-conserved reaction:

$$17 \text{ Liz/Chr} = \text{Atg} + 3 \text{ Br} \qquad (1)$$
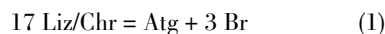
(see Table 1 for a complete list of reactions and abbreviations). This reaction may be inferred to account for the change, widely observed in prograde metamorphism, by which pre-existing chrysotile and lizardite, in many instances still with pseudomorphic texture, are overgrown by blades of antigorite (e.g., Springer, 1974; Frost, 1975; Vance and Dungan, 1977; Pinsent and Hurst, 1977; Wicks and Whittaker, 1977; Evans, 1977; Maltman, 1978; Wicks and Plant, 1979; Brown et al., 1982; Ikin and Harmon, 1983; Igarashi et al., 1985; O'Hanley et al., 1989; and many others). Progress of this reaction may be smeared out over a large range of temperature conditions, even in regional metamorphism (Trommsdorff, 1983; Mellini et al., 1987). Applicable in some cases perhaps is the alternative possibility of a modest introduction of SiO_2 to convert lizardite/chrysotile to antigorite (e.g., Coleman, 1971; O'Hanley, 1991; O'Hanley and Wicks, 1995), below or metastably above the temperature of reaction 1, as in coarsely columnar antigorite (Jahns, 1967), such that brucite is not formed as a byproduct:

$$16 \text{ Liz/Chr} + 2 \text{ SiO}_{2,\text{aq}} = \text{Atg} + H_2O. \qquad (2)$$
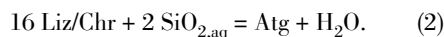
After completion of reaction 2, further SiO_2 introduction generates talc and converts any diopside present to tremolite, another asbestos mineral (Williams-Jones et al., 2001).

In regional and most cases of contact metamorphism, antigorite is from then on the stable serpentine mineral leading upgrade in metaperidotites to the paragenesis forsterite + talc (Trommsdorff and Evans, 1972), or in very high-pressure metamorphism, to forsterite + enstatite (Trommsdorff et al., 1998). Field, isotopic, and laboratory evidence are in agreement in characterizing antigorite as the high-temperature form of Mg-serpentine, corresponding to formation temperatures in the range of ~ 250°C to more than 500°C (Wenner and Taylor, 1971; Evans et al., 1976; Chernosky et al., 1988; O'Hanley, 1996).

The retrograde formation of antigorite from olivine, which in its simplest form is the reaction:

TABLE 1. Serpentine Equilibria Mentioned in the Text

1. 17 Liz/Chr = Atg + 3 Brc

2. 16 Liz/Chr + 2 SiO$_{2, aq}$ = Atg + H$_2$O

3. Atg + 20 Brc = 34 Fo + 51 H$_2$O

4. Atg = 18 Fo + 4 Tlc + 27 H$_2$O

5. Complex system mass balances

6. Liz/Chr + Brc = 2 Fo + 3 H$_2$O

7. 20 Chr/Liz = Atg + 6 Fo + 9 H$_2$O

Key

Liz/Chr	Mg$_3$Si$_2$O$_5$(OH)$_4$	Lizardite/Chrysotile
Atg	Mg$_{48}$Si$_{34}$O$_{85}$(OH)$_{62}$	Antigorite
Fo	Mg$_2$SiO$_4$	Forsterite
Tlc	Mg$_3$Si$_4$O$_{10}$(OH)$_2$	Talc
Brc	Mg(OH)$_2$	Brucite

$$34 \text{ Fo} + 51 \text{ H}_2\text{O} = \text{Atg} + 20 \text{ Br} \qquad (3)$$

has been reported in a number of places (e.g., Peacock, 1987; Wicks and O'Hanley, 1988, p. 141; O'Hanley et al., 1989; O'Hanley and Dyar, 1993), but it is far less widely observed than the pseudomorphic hydration of peridotite to lizardite[1]. Retrograde antigorite may well be abundant in forearc upper mantle, due to the influx of H$_2$O released from the subducted slab below (Peacock, 1993: Guillot et al., 2000). Hydration of peridotite in this location is inferred from anomalously low shear-velocities in seismic profiles (Bostock et al., 2002; Brocher et al., 2003).

Internally consistent thermodynamic evaluations of MSH minerals (not including lizardite), using virtually the same experimental dataset available to Evans et al. (1976), were made later by Helgeson et al. (1978), Trommsdorff (1983), Day et al. (1985), and Berman (1988). Evans et al. (1976) emphasized field data relevant to reaction 1 that, at the same time, allowed satisfactory fitting of the experimental reversals of chrysotile and antigorite breakdown reactions. Helgeson et al. (1978) considered solubility data as well as phase-equilibrium constraints,

and concluded that chrysotile was less stable than antigorite at all pressures and temperatures. Trommsdorff (1983) found that the thermal limit of chrysotile with respect to antigorite was at too low a temperature to match the field evidence. The "least deviation" dataset of Day et al. (1985) also indicated no stability field for chrysotile, although these authors stressed the uncertainty of that conclusion. Berman (1988) used principally the results of bracketed phase-equilibrium experiments to derive by mathematical programming a set of internally consistent thermodynamic data for chrysotile, antigorite, and other minerals in the MSH system, and his data have been widely used. Reaction 1 for chrysotile was calculated by Chernosky et al. (1988) using the optimized data of Berman (1988) to be a steep line with negative slope in the PT diagam between 200 and 260°C, about 100°C lower than estimated by Evans et al. (1976).

More recent phase-equilibrium bracketing experiments (Khodyrev and Agoshkov, 1986; Ulmer and Trommsdorff, 1995; Wunder and Schreyer, 1997; Bromiley and Pawley, 2003) have sought to determine the limit of stability of antigorite under the PT conditions of subduction zones. With the release of as much as 12 wt% H$_2$O, the breakdown of MSH-antigorite, with a maximum temperature of ~640°C at 20 kbar (several tens of degrees higher for Al-antigorite), has great relevance to a possible earthquake source mechanism in the slab, and to

---

[1]Note that in prograde metamorphism, platy antigorite in textural equilibrium with granular olivine appears to pierce the olivine in a manner that could be erroneously thought the result of replacement of olivine by antigorite.
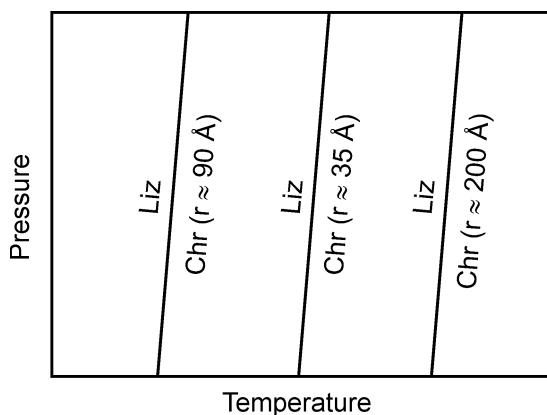
FIG. 1. Possible P-T relations of lizardite and chrysotile composed of variable integrated radii.

potential magma generation in the mantle wedge above. Although these experiments suggest no need for revision of the low-pressure breakdown curve for antigorite (Evans et al., 1976), additional bracketing experiments below 10 kbar with contemporary phase characterization techniques, and preferably in the pure system MSH, would still be useful, given its importance for the calculated location of reaction 1.

In graphical terms, the PT line for reaction 1 emerges from an invariant point where three dehydration reactions meet at acute angles of intersection. As a result, the location of 1 has an uncertainty in terms of T or P that is an order of magnitude larger than the locations of the experimentally bracketed dehydration reactions from which the optimized thermodynamic properties were largely derived. For example, an optimistic ± 10°C uncertainty in the determination of the breakdown reaction of antigorite:

$$Atg = 18 \, Fo + 4 \, Tlc + 27 \, H_2O \qquad (4)$$
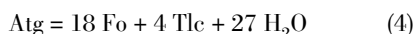
translates at 1–2 kbar into an error of ± 125 to 135°C in the location of reaction 1.

Many factors have been and may be suggested as contributing to uncertainties in the MSH mineral database at low temperature, in addition to interlaboratory differences. They include: (1) use of different starting materials (synthetic products vs. impure minerals); (2) inadequate phase characterization (polymorphic and polytypic uncertainties including possible transformations during the experiments and unrecognized lizardite growth from olivine in

the experiments on chrysotile); and (3) non-recognition of polysomatism in antigorite (the wrong m-value for the experimental PT conditions). These problems are magnified when propagated into the calculation of reaction 1, whose PT location is important in the context of a possible stability field for chrysotile vis-à-vis lizardite.

Relative Stability of Chrysotile and Lizardite: Field Evidence

If we accept that the thermodynamic properties of cylindrical chrysotile depend on an integration over the range of radii present, then equilibrium with its dimorph lizardite should be considered pseudo-divariant rather than univariant, with chrysotile most stable for the minimum-energy radius and least stable when a maximum of undercurved outer layers and overcurved inner layers is present (Fig. 1). The variance is "pseudo" because the stable boundary for dimorphs must be univariant in the system MSH, corresponding to the definition of standard states. In this model, we should not expect the Gibbs free energy of pure chrysotile to have a unique value when measured, for example, by different techniques and using different starting materials. Perhaps nature reflects this variability in a corresponding manner?

Where, if anywhere, do we place lizardite in the P-T diagram, and what does this do to the field of chrysotile? Bracketed reactions of lizardite analogous to those supposedly involving chrysotile have not explicitly been investigated experimentally. The field evidence is unfortunately complicated by the

widely observed intimate coexistence of polytypes of both lizardite and chrysotile in the same rock, and in some cases antigorite as well (Cressey and Zussman, 1976; Cressey, 1979; Wicks and Plant, 1979; Veblen and Buseck, 1979; Wicks and O'Hanley, 1988; O'Hanley and Wicks, 1995; Viti and Mellini, 1998). The sluggish kinetics of reactions among the serpentine minerals in nature is in significant contrast to the rates of hydration of olivine, and the converse, found in the laboratory under H_2O saturated conditions (e.g., Martin and Fyfe, 1970; Wegner and Ernst, 1983). The field evidence provides seemingly contradictory indications of the relative stability of chrysotile and lizardite. Nevertheless, the field evidence is illuminating in that it shows that different processes are involved in their crystallization, and an understanding of these processes provides some explanations for the contradictions. The reader is forewarned here that we shall conclude that bulk chrysotile has no stable field of existence (see the section on laboratory evidence below).

Estimates of the formation temperatures of chrysotile- and lizardite-bearing serpentinites in nature range from surface or near-surface temperatures to temperatures in excess of 300°C. Oxygen-isotope fractionations between serpentine and magnetite mostly indicate lower values in this range for lizardite (O'Hanley, 1996, and citations in Viti and Mellini, 1998). Despite the broad overlap in growth conditions, consistent differences are found to exist in the modes of occurrence of lizardite and chrysotile. Most lizardite serpentinites in the geologic record formed by the direct hydration of peridotite at low temperature (O'Hanley, 1996). Chrysotile serpentinites and chrysotile asbestos are best developed in serpentinites that have undergone some recrystallization, most commonly under conditions approaching or within those associated with the greenschist facies. The differences in mode of occurrence seem to hold true no matter what the temperature. For example, the alteration of olivine to lizardite under zeolite-facies conditions was reported in serpentinite fanglomerate by Cashman and Whetten (1976), and asbestiform chrysotile veins were found to have formed in the porous matrix of a debris flow of Quaternary age (Craw et al., 1987). At the other extreme, there are indications of the survival of both lizardite and chrysotile to temperatures probably in excess of 400°C.

Lizardite formation in nature

The geologic environments most productive of lizardite are those where H_2O can gain access to peridotite along joints, fractures, faults, and shear zones beneath the land surface or sea floor, and initiate hydration. The kinds of water involved (oceanic, meteoric, metamorphic, igneous, connate) are as diverse as the tectonic environments in which serpentinization of peridotite takes place. More or less orthogonal fractures may have been induced by thermal contraction in the peridotite prior to serpentinization. Early stages of alteration are characterized by pseudomorphic textures, such as mesh and hourglass serpentine replacements of olivine and bastite serpentine replacements of pyroxenes, amphiboles, and sheet silicates, through which protolith minerals and textures can usually be readily identified (Wicks and Whittaker, 1977; Wicks et al., 1977; Wicks, 1984a). Mesh rims are typically composed of an orthogonal arrangement of parallel pseudofibers of lizardite-$1T$ that are optically length fast (α-serpentine). Serpentine mesh centers, which logic would suggest form later than mesh rims, tend to be more complex mineralogically (Cressey, 1979; Wicks and O'Hanley, 1988; Viti and Mellini, 1998), and include lizardite-$1T$ (α-serpentine), chrysotile, polygonal serpentine, and antigorite (γ- or isotropic serpentine). In metadunites, in addition, small amounts of brucite may be present. Bastite pseudomorphs are composed predominantly of lizardite. The local presence of Al, Cr, and Fe^{3+} no doubt provides a favorable compositional environment for lizardite in bastite (e.g., Dungan 1979a). Unfortunately, we generally have little information about the temperatures of most examples of lizardite serpentinization events in nature. Some writers have questioned whether oxygen isotope analyses of separates of coexisting serpentine and magnetite can be taken as representative of equilibration during a single event.

Evidence is compelling (constant whole-rock element ratios, microstructures, kernel structure) that the hydration reaction may be accompanied by volume expansion, on the order of 40–50% (Hostetler et al., 1966; Bogolepov, 1970; Coleman and Keith, 1971; O'Hanley, 1992). This will tend to seal up pathways of infiltration and diffusion at or close to the reaction site itself, resulting in an extremely rock-dominant environment. Away from the reaction site, the expansion induces secondary cracks. Thus, the expansion may manifest itself on the scale of single olivine crystals as seen
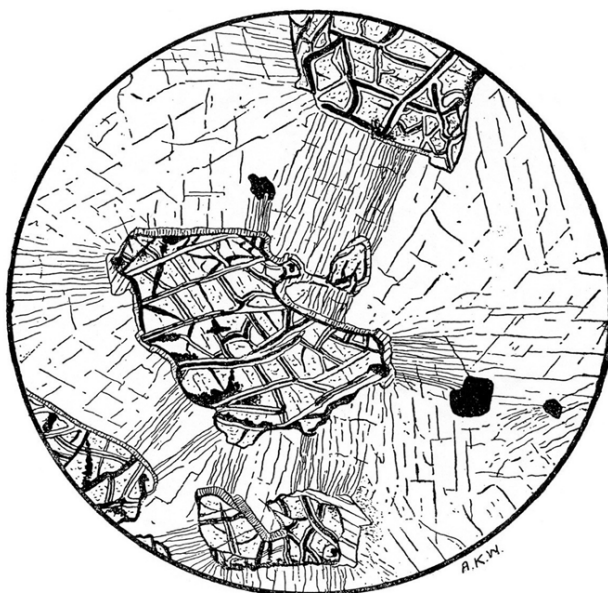
FIG. 2. Olivine veined by serpentine with separation of magnetite, in plagioclase traversed by systems of closely spaced fractures. A thin veneer of orthopyroxene surrounds the olivines, which measure 2–3 mm. Troctolite, Belhelvie, Aberdeen, Scotland. From Hatch et al. (1949).

for example in troctolite (e.g., Hatch et al., 1949, Fig. 114; Fig. 2 this paper), where cracks radiate out into the surrounding plagioclase, or on the outcrop scale as in the kernel structures described by O'Hanley and Offler (1992) and O'Hanley (1992; Fig. 3 this paper). Note in Figure 2 how the tension cracks mostly originate from the tip regions of the olivine where stress concentrations would be expected. Differential elastic strains resulting from cooling, on the other hand, produce concentric fractures in the surrounding plagioclase (Van der Molen and Roermund, 1986, Fig. 1A).

The volume behavior of serpentine replacement of olivine in massive peridotite is at odds with overwhelming textural evidence from numerous geologic environments, including metamorphic ones, for mineral replacements, especially those involving hydration, to take place with constant volume of solids (Merino and Dewers, 1998). Volume conservation has been shown to apply to serpentinite-related processes such as rodingitization and formation of chloritic blackwall (Puschnig, 2002). Volume increase during serpentinization means either that the host ultramafic has low viscosity, or, much more likely, that the necessary mass transfer required for volume conservation (diffusion out of Mg mostly, but also some Si) was limited. The high-pH aqueous fluid emerging from partially or un-serpentinized peridotite at low temperature contains very little Mg (Barnes et al., 1978). However, where a steep chemical potential gradient for Mg might exist, such as in a small body of ultramafic rock enclosed in siliceous country-rock, or in a high water/rock environment, or in sheared serpentinite, original volumes might be better preserved during serpentinization. On the other hand, an appropriate potential gradient for diffusive loss of Si from serpentinite is distinctly implausible (Hostetler et al., 1966). The truth lies somewhere between the constant-volume model (Thayer, 1966) and the constant-composition model (Hostetler, et al., 1966), and it depends on the occurrence (Coleman, 1971). Bogolepov (1970) noted that Soviet geologists working in areas of local serpentinization believed in volume conservation, whereas those working on regional serpentinites favored volume increases.

The coexistence of relict olivine and lizardite (± brucite) at low temperature defines low values of water activity along crystal contacts (e.g., Sanford, 1981; MacDonald and Fyfe, 1985). This should create a strong potential gradient for water to penetrate to the site of reaction. As the rate of reaction is not

the rate-limiting step except at very low temperatures (Martin and Fyfe, 1970; Wegner and Ernst, 1983), the widespread occurrence of arrested serpentinization means either that water was not available in neighboring cracks or that permeability was too low (perhaps limited to little more than defects in the lizardite structure according to MacDonald and Fyfe, 1985). In either case, we can conclude that peridotite hydration commonly takes place sluggishly in a very dry or largely solid-state environment, one that we inferred earlier favors lizardite over chrysotile. The common inheritance of oxygen isotope compositions from precursor minerals is consistent with low water/rock ratios for the serpentinization process (Barnes et al., 1978; Burkhard and O'Neil, 1988).

The expansion that accompanies the serpentinization of peridotite has to be attributed to the force of crystallization of the hydrous products, predominantly lizardite. This force is probably most effectively delivered along [001] of lizardite. The extraordinary feature of α-oriented lizardite is that elongation is normal to the sheet structure, unlike almost all other sheet silicates. Viti and Mellini (1998) showed by TEM that the axis of the hexagonal pyramids/cones that constitute the α-serpentine pseudofibers in mesh rims (and hourglass texture) are oriented normal to the mesh rim boundary and to the basal cleavage, with a polarity such that they point inwards (Fig. 4). They interpreted this microstructure in terms of nucleation and growth into the olivine. One has to wonder if crystallization or recrystallization under expansion stress could be responsible for this microstructure, and also the hourglass texture? Cressey (1979) interpreted the elongate stacking of lizardite plates as due to recrystallization. Normand et al. (2002) found 7 Å serpentine in the form of conical structures in their reaction products, but in these the layers are packed parallel to the cone walls rather than normal to the cone axis (C. Normand, pers. commun., December 2003).

Chrysotile cannot exert a force of crystallization except possibly parallel to its cylinder axis, and for this reason as well as others, it is an unlikely product of direct olivine hydration in nature. In her study of ophiolites from the ocean floor, Prichard (1979) concluded that lizardite formed from olivine and that chrysotile only grew after olivine was eliminated. Similar conclusions were made by Laurent and Hébert (1979) and Cogulu and Laurent (1984) for the serpentinites of southeastern Quebec. These
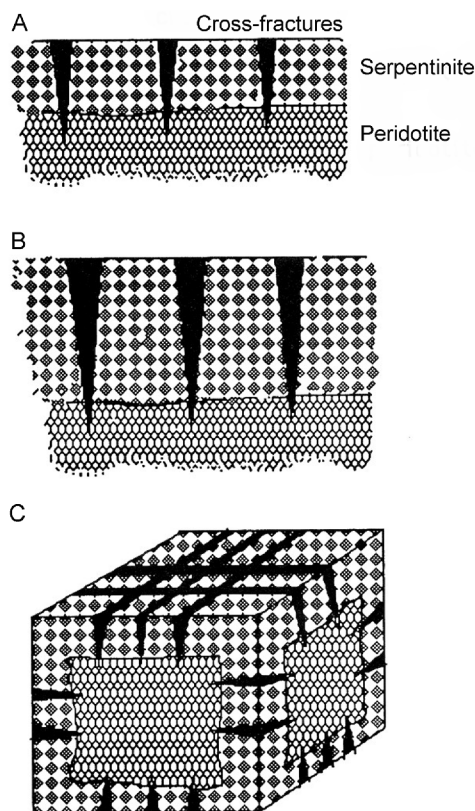

FIG. 3. Diagram illustrating the development of outcrop-scale kernel pattern and cross-fractures during serpentinization of peridotite, from O'Hanley (1992). Cross-fractures widen and lengthen with progressive serpentinization of the interior peridotite.

observations are consistent with expansion and low porosity and permeability while olivine was reacting to lizardite, and the opening of pore spaces following the completion of hydration. The microstructures produced during the expansion phase have certain analogies with the fibrous palisade quartz and radiating cracks associated with the decompression reaction of coesite to quartz (Chopin, 1984; Chopin et al., 1991; Hacker and Peacock, 1995). The PdV work done by lizardite and brucite is in lieu of some of the potential heat evolved by the reaction (e.g., Fyfe, 1990), but the fraction of heat lost in this manner is small except possibly at high pressures, for example in the forearc mantle.

An essential feature of the kernel model for expansion (O'Hanley, 1992, 1996) is the development of radiating cracks in fully serpentinized
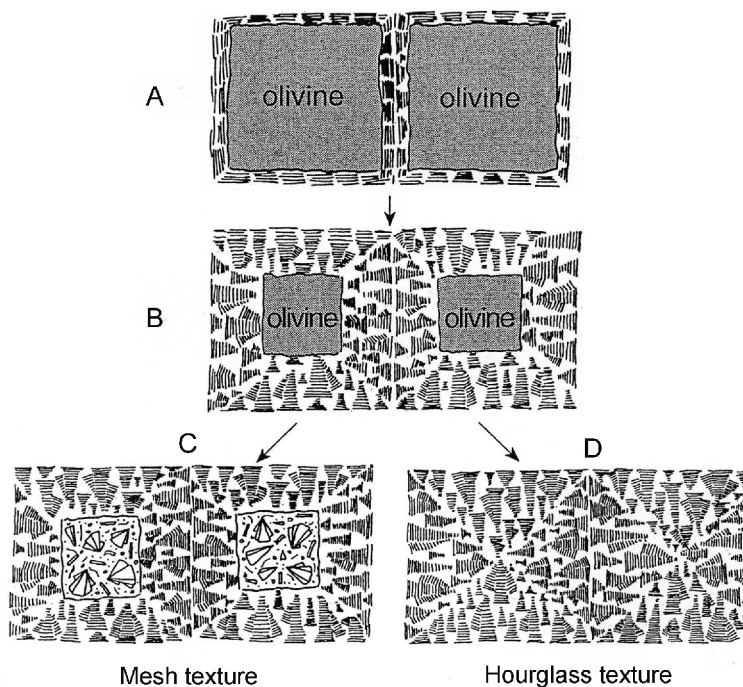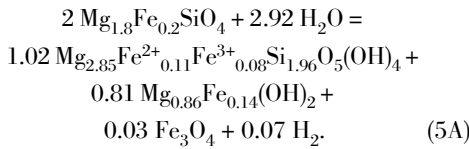
FIG. 4. Microscopic view of the hydration of olivine to serpentine, from Viti and Mellini (1998). Mesh rims consist of a three-dimensional growth of lizardite (alpha orientation) as steep hexagonal pyramids or cones with an inward-pointing polarity.

peridotite immediately surrounding the kernel that is simultaneously undergoing active serpentinization. The field association of asbestos veins with this transition was noted long ago by Bain (1932) and Cooke (1936) in the asbestos mines of Quebec. In these cases, we must consider the formation of chrysotile in veins to be basically contemporaneous (same T and P) with the growth of the lizardite that causes the kernel peridotite to expand.
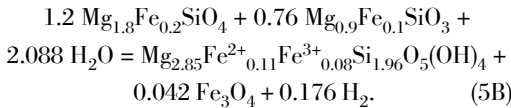
In serpentinized dunites and harzburgites with the typical Fo_{90} olivine, lizardite (especially when pseudomorphic) has compositions that are frequently close to ~94–95% of the Mg end-member, or even higher if projected Al-free (Hostetler et al., 1966; Page, 1966; Dungan, 1979b; Wicks and Plant, 1979; Cogulu and Laurent, 1984; Peacock, 1987; O'Hanley and Dyar, 1993; Viti and Mellini, 1998). The remaining 5–6% consists mainly of Al, Fe^{2+}, and Fe^{3+} end-members. These signs of Fe/Mg fractionation between lizardite and olivine suggest that the products of the serpentinization reaction are influenced by the $MgFe^{-1}$ exchange potential of the host

olivine. Antigorite has a smaller $(\Sigma Fe)/Mg$ ratio than coexisting olivine in equilibrium-textured antigorite-olivine rocks such as the Malenco serpentinite (Trommsdorff and Evans, 1972; Worden et al., 1991; Peretti et al., 1992), and it is likely that a similar kind of partition holds for lizardite and olivine. Therefore, the Mg-rich nature of the serpentine minerals in metaperidotites is not a consequence of an oxidation reaction, but the result of a tendency to be in local exchange equilibrium with olivine. This equilibrium may not hold initially (Baronnet and Boudier, 2001), but it seems to improve with recrystallization and further hydration (Toft et al., 1990). In the assemblage olivine + lizardite + brucite + magnetite, the chemical potentials of all components are theoretically fixed in an isobaric and isothermal system (C = 5, FMSHO; P = 5, Ol, Liz, Brc, Mag, Fluid). As long as H_2O can infiltrate and heat escape, lizardite, brucite, and magnetite should grow with ideally constant compositions. Making the reasonable assumption of oxygen conservation (see below), the reaction in a dunite might be written as follows:

$$2\,Mg_{1.8}Fe_{0.2}SiO_4 + 2.92\,H_2O =$$
$$1.02\,Mg_{2.85}Fe^{2+}_{0.11}Fe^{3+}_{0.08}Si_{1.96}O_5(OH)_4 +$$
$$0.81\,Mg_{0.86}Fe_{0.14}(OH)_2 +$$
$$0.03\,Fe_3O_4 + 0.07\,H_2. \qquad (5A)$$

The greatest uncertainty in this reaction is the choice of an appropriate composition for brucite.

In a metaharzburgite, the Phase Rule constraints will still apply, but for SiO_2 mass balance, instead of brucite we will have talc or, more commonly, metastable enstatite, for example:

$$1.2\,Mg_{1.8}Fe_{0.2}SiO_4 + 0.76\,Mg_{0.9}Fe_{0.1}SiO_3 +$$
$$2.088\,H_2O = Mg_{2.85}Fe^{2+}_{0.11}Fe^{3+}_{0.08}Si_{1.96}O_5(OH)_4 +$$
$$0.042\,Fe_3O_4 + 0.176\,H_2. \qquad (5B)$$

Labotka and Albee (1979) wrote an analogous reaction for antigorite serpentinization. In fact, dozens of possible serpentinization reactions may be found in the literature (e.g., the compilation in Toft et al., 1990). A comparison of reaction 5A with 5B suggests that serpentinization of harzburgite will produce more magnetite (e.g., Coleman and Keith, 1971) and H_2 than dunite. In reaction 5B, without adding O_2, the "whole-rock" ratio Fe^{3+}/Fe^{2+} has gone from zero to >1.0. Ratios larger than 2.0 (e.g., Viti and Mellini, 1998) imply more Fe^{3+} than Fe^{2+} in lizardite and/or the presence of hydroandradite.

If lizardite serpentinization is accompanied by falling temperature or pressure, the Phase Rule constraints will be relaxed; most important, the H_2O activity will decline with falling temperature, whereas mineral compositions may show little change since the K_D constraints are robust. Of course, to the extent that with reaction progress the domain of equilibrium no longer encompassses all the required phases, changes may occur in the compositions of the minerals, iron-enrichment for example.

The oxygen to convert Fe^{2+} in olivine to Fe^{3+} in magnetite and lizardite comes from dissociation of the H_2O (Moody, 1976; Frost, 1985). Hydrogen generation during serpentinization (e.g., Thayer, 1966; Barnes et al., 1972; Coveney et al., 1987; Abrajano et al., 1990) supports the oxygen-conserved and rock-dominant nature of lizardite serpentinization, and is consistent with calculations of low redox states (e.g., Frost, 1985; Abrajano et al., 1990) and the common occurrence of native metals, notably Ni-Fe alloys, in lizardite and antigorite parageneses (Hostetler et al., 1966; Eckstrand,

1975; Frost, 1985; Rossetti and Zucchetti, 1988; Peretti et al., 1992). A seemingly strange, but perfectly reasonable feature of many serpentinites is the equilibrium coexistence of the ferric (magnetite, hydro-andradite), ferrous, and native states of iron. When carbon is present in the system, the low-redox conditions account for the presence of abiogenic methane as well as hydrogen in the fluid generated by serpentinization (e.g. Abrajano et al., 1988; Bernt et al., 1996; Schroeder et al., 2002) and the precipitation of graphite in serpentinized olivine (Pasteris, 1981). Dilution of H_2O by CH_4, H_2, and H_2S in the fluid phase attending serpentinization can shift the hydration reactions down temperature by several tens of degrees (Früh-Green et al., 2004). Hydrogen produced by serpentinization should be distinguished from hydrogen in low-temperature hot-springs (e.g., Neal and Stanger, 1983), which may be derived by weathering of the Fe^{2+}-bearing minerals of serpentinite. The occurrence of very magnesian olivine (Fo_{93-98}) in metaperidotite formed by deserpentinization (Vance and Dungan, 1977; Nosaka, 2003) shows that the Fe^{2+} and Fe^{3+} in magnetite are not readily returned to olivine by a reversal of reactions 5A or 5B, no doubt because that would require a reintroduction of hydrogen.

Reactions 5A and 5B are strongly exothermic (~ 35 kJ/mol H_2O) and have relevance to the heat budget of the ocean lithosphere (MacDonald and Fyfe, 1985; Fyfe, 1990; Lowell and Rona, 2002). They are inferred to be the source of heat driving non-volcanic, off-axis hydrothermal activity that in turn creates chimneys of aragonite, calcite, and brucite on the ocean floor (Kelley at al., 2001), and provides ideal conditions for microbial communities in subsurface and near-vent environments (Früh-Green et al., 2004). Chrysotile may be more abundant than lizardite in such convective hydrothermal systems.

Chrysotile formation in nature

Chrysotile has been reported in both rims and cores of mesh-textured serpentinite (Cressey, 1979; Wicks and Plant, 1979; Wicks and O'Hanley, 1988; Viti and Mellini, 1998). However, it is far less common there than lizardite, and is believed to represent growth following the initial hydration (O'Hanley, 1996). From numerous field descriptions, it is clear that chrysotile occurs preferentially in serpentinites that have undergone some degree of recrystallization, in which the serpentine minerals have begun to form interlocking textures. It is

generally less clear whether the driving force for this recrystallization is an increase in temperature, or the onset of deformation opening cracks that can hold aqueous fluid and serve as pathways for the movement of fluids, or possibly both. Most typically, chrysotile grows as vein-fillings of cross-fiber and slip-fiber, and but it also occurs in serrate veinlets formed by replacement. In some cases, the serrate veinlets are sufficiently pervasive that the term mass-fiber asbestos is more appropriate. At the nano-scale, chrysotile may be seen to fill voids opened up, for example, by deformation of host lizardite. Recrystallization is not the appropriate term for the formation of most chrysotile in nature.

In the process of hydration of peridotite, lizardite appears to possess at least two advantages over chrysotile that are not related to their relative Gibbs free energies: (1) heterogeneous nucleation and growth of lizardite potentially benefits from crystal structure similarities with reactant chain and sheet silicates, if not olivine; (2) lizardite's capacity to exert a force of crystallization contrasts with that of chrysotile whose growth and existence seem to demand fluid-filled voids and isotropic stress. Would it be wrong to view lizardite and chrysotile as a stress-antistress mineral pair? Maltman (1978) described the recrystallization of mesh lizardite under shearing stress to ribbons of lizardite (alpha serpentine). Wicks (1984b) reported that foliated chrysotile is usually the dominant serpentine mineral in shear zones in low-temperature serpentinites showing both brittle and ductile behavior. However, in some cases, he describes it as non-fibrous chrysotile and in others as Povlen type (polygonal) chrysotile. Tectonic flattening of chrysotile cylinders results in nucleation and growth of chrysotile of energetically more appropriate radii, and growth of lizardite (Baronnet and Devouard, 1996). Extreme flattening of chrysotile seems likely to yield a planar serpentine (lizardite, or antigorite at higher temperatures) that can accommodate shear stress by slip along (001). The strongly foliated "chrysotile" in intensely sheared zones would be a good subject for further TEM investigation.

For the above reasons we might suppose (for the moment) that the prevalence of lizardite over chrysotile in retrograde, hydrated peridotite derives not from its greater stability in the conventional sense, but from circumstances of growth that discriminate against chrysotile: the scarcity of H_2O, absence of void space, nucleation advantages, and the presence of stress related to expansion. When the advantages

for lizardite crystallization are not present, as in fluid-filled pores and cracks, the predominant form of serpentine mineral at low temperature becomes chrysotile.

If, on the other hand, as the experimental data in MSH indicate (see below), chrysotile is thermodynamically less stable than lizardite under the PT conditions generally assumed for chrysotile vein-formation, then we have to explain why lizardite is not more prominent in veins. In many cases, lizardite is present in the serpentinite hosting the chrysotile vein, although in some instances it is predominantly antigorite. What advantage (kinetic? compositional?) does chrysotile apparently possess over lizardite to aid its growth in fluid-filled cracks and other voids? By analogy with the ease of growth of chrysotile in the laboratory from high free-energy oxide and gel starting materials, it is reasonable to think in terms of oversaturation of the fluid in Mg and Si in nature as well. Under circumstances of significant permeability (open-system behavior, high water-rock ratio), we would expect diminished buffering control of solute concentrations in the fluid by the MSH minerals in the immediately adjacent rock. Effective rates of nucleation and growth of serpentine minerals may be rapid, and no longer limited by the slow diffusion of H_2O. But we have to remember that supersaturation alone, beyond the solubility product of chrysotile, no matter how long that condition prevails (Normand et al., 2002), will affect the ΔG_v (for nucleation) and molar ΔG_r (for growth) of chrysotile and lizardite equally. In these environments, chrysotile may simply have a higher intrinsic growth rate than lizardite under the same conditions. Several geological processes can be invoked to cause local supersaturation, for example, down-temperature fluid flow, down-pressure fluid flow (dilatancy pumping), fluid mixing, and fluid equilibration with metastable minerals, or it may be a natural consequence of microporosity (e.g, Putnis, 2002) or local heterogeneities in chemical potentials. These processes call upon both infiltration and diffusion of H_2O, and we don't know which prevails in the case of chrysotile growth.

Cross-fiber chrysotile occupies subparallel or en-echelon sets of veins that have sharp edges and matching parallel sides indicative (ordinarily) of dilation, and lack a selvage of alteration (Wicks and O'Hanley, 1988). They have been interpreted as representing zones of relative tension (Zoltai, 1981) and shown to be kinematically linked to nearby faults (Cooke, 1936; O'Hanley, 1988). Fibers are

believed to track the relative displacement of opposing walls and thus have potential for recording incremental strain vectors. Veins typically terminate after several meters, and do not extend into country rock; some occur sufficiently regularly spaced as to suggest self-organization. They are characteristically monomineralic or nearly so, and accessory minerals (such as magnetite forming a median line) tend to reflect those in the host-rock (Cogulu and Laurent, 1984). The sense of growth seems to fit the criteria for antiaxial fiber veins (Ramsay and Huber, 1983). These observations are compatible with a fluid chemistry (ion activity product) controlled by serpentinite, even though stable isotopes and trace constituents may in some instances indicate a foreign source for the fluid (O'Hanley, 1996).

The generally accepted crack-seal growth model for fibrous veins (Ramsay and Huber, 1983) accounts for preferential shape orientation but not for preferred lattice orientation. It applies to veins of calcite, quartz, and gypsum, etc. that are not fibrous when they grow hydrothermally. Rather than fracturing and fluid-flow, an alternative model for fibrous veins (Bons and Jessell, 1997) that resolves some of the problems of crack-seal growth involves diffusional transport driven by dissolution-precipitation creep, but this model also predicts fiber shapes that are unrelated to crystallographic orientation. These models clearly need to be refined or modified to account for chrysotile cross-fiber veins (and similar cross-fiber veins elsewhere composed of chain silicates such as tremolite, anthophyllite, and crocidolite). Wiltschko and Morse (2001) argued for crystallization pressure following crack opening as a mechanism for banded fibrous veins. However, Baronnet and Belluso (2002) pointed out that sharp bends in fiber orientation are not pristine kink-band boundaries, and that serpentine-wall contacts are loose. In another model, we might envisage that fibers growing (anisotropically) parallel to the opening direction might possess a statistical advantage over those at an angle to it because the latter are more likely to blocked by impinging on a neighboring fiber. By this model, parallelism of fibers should be least good at the start of vein growth, that is, close to the median line in an antiaxial vein.

Whatever the actual mechanism, growth of slip-fiber chrysotile is fundamentally no different from that of cross-fiber chrysotile, except that in the former extension is parallel to the slip plane and fluid occupies voids associated with periodic jogs, steps, or risers in the structure. Fiber growth linea-

tions are just one class of slickenside lineation, in which mineral fibers grow in slowly dilating potential voids on fault surfaces (Durney and Ramsay, 1973; Means, 1987). The mineral lineation so formed will superficially resemble extensional mineral lineations formed by crystal-plastic deformation. Slip-fiber chrysotile has been reported as having formed in some cases by realignment of cross-fiber chrysotile during later shearing, or even destroyed when the shearing was intense (Skarpelis and Dabitzias, 1987; O'Hanley, 1987).

The critical factor for chrysotile growth may perhaps not be a certain degree of supersaturation, but simply the presence of porosity that permits the unrestrained growth of chrysotile cylinders composed of low-strain layers (initially as "Roman tiles" a few layers thick; Baronnet and Devouard, 1996). Such layers may be intrinsically more stable than lizardite (i.e., we are in the pseudo-divariant region, Fig. 1). Growth of increasingly more strained, higher-energy inner and outer layers of chrysotile represents a kinetically easy growth path, in a fluid that is mildly supersaturated with respect to both lizardite and chrysotile. With the passage of time, the chrysotile may spontaneously evolve to polygonal serpentine and subsequently to ordinary lizardite (Viti and Mellini, 1997), or even be replaced by antigorite. Preferential growth of chrysotile vs. lizardite seems to come down to nucleation and growth rates in their different environments: for chrysotile, high water-rock ratios, modest supersaturation, and growth from fluid; for lizardite, low water-rock ratios, low supersaturation, growth by hydration of olivine, pyroxene, etc., and stability under non-isotropic stress. It is not obvious that this offers an explanation for chrysotile in serrate veins and mass-fiber deposits, however.

For indications of relative stability in the classical thermodynamic sense based on nature, we have to focus on the evidence for polymorphic transitions among the serpentine minerals that can be inferred to have occurred as a spontaneous process (loss of Gibbs free energy) in response to changes in the values of the intensive properties of the system. For this we need unambiguous evidence not only of their relative time of growth, but also evidence of *in situ* replacement, preferably pseudomorphic, approaching closed-system behavior. A supersaturated fluid can deposit a mineral that is metastable, but the same fluid cannot simultaneously dissolve a more stable polymorph isochemical with (or in exchange equilibrium with) the first. Only a more complex

process, involving open-system behavior, can result in the appearance and growth of a less stable polymorph.

Based on field and microscopic observations there are many claims in the literature for the replacement of lizardite by chrysotile in some places, and the replacement of chrysotile by lizardite in others (O'Hanley, 1996). The very fine scale of most serpentine microstructures unfortunately means that only in unusually favorable cases can the case for *in situ* replacement be made with certainty with the unaided eye or under the polarizing microscope.

Among the more convincing examples of the formation of lizardite at the expense of chrysotile is the replacement of chrysotile veins by lizardite (e.g., at Cassiar, British Columbia, O'Hanley, 1988; O'Hanley and Wicks, 1995; and Garrison, Ontario, O'Hanley, 1991). TEM study has shown that this transition usually involves polygonal serpentine at an intermediate stage (Baronnet and Devouard, 1996; Viti and Mellini, 1997). The field term "picrolite" describes this pseudo-fibrous material, although further investigation has often revealed the presence in it of antigorite and other minerals. However, we have to be sure that these replacements are not driven by compositional changes. For example, the vein lizardite on Elba is richer in Fe and Al than the earlier vein chrysotile it replaced (Viti and Mellini, 1997). On the other hand, in the Garrison asbestos deposit, chrysotile has much the same composition as the lizardite it replaced (O'Hanley, 1991).

How likely is possible stabilization of lizardite relative to chrysotile, and vice versa, to be the result of additional components such as Fe^{2+}, Fe^{3+}, and Al? In this context one notes that: (1) both lizardite and chrysotile have been synthesized in the pure MSH system; (2) compositions with more than 99% $Mg_3Si_2O_5(OH)_4$ have been found in nature for both lizardite and chrysotile, especially, but not exclusively, in magnesian marbles (e.g., lizardite in metadunite, sample 18491, Wicks and Plant, 1979; lizardite in marble, sample M19804, O'Hanley and Dyar, 1993; chrysotile in marble, Nagy and Faust, 1956); (3) there is much overlap in the chemical compositions of natural lizardite and chrysotile at the low Al and Fe end (Page, 1968; Whittaker and Wicks, 1970; Frost, 1975; Chernosky, 1975; Wicks and Plant, 1979; Dungan, 1979b; O'Hanley and Dyar, 1993; Viti and Mellini, 1997), especially if one compares compositions of rock-forming chryso-

tile and lizardite in individual occurrences of metadunite and metaharzburgite, and excludes bastites. We know that there is a preference of lizardite for Al and Fe^{3+} (Caruso and Chernosky, 1979; O'Hanley and Dyar, 1993), and, according to O'Hanley and Dyar (1998), a preference for Fe^{2+} in chrysotile, and there is reasonable crystal-chemical logic for these preferences. However, quantitative assessments of systematic partitioning are subject to unavoidable limitations on the sample population, and do not represent mineral pairs in close contact where exchange equilibrium might have existed. They do not justify the conclusion that chrysotile and lizardite are not polymorphs in nature; differential uptake of minor constituents is normal in virtually all mineral polymorphs.

The case for significant impurity stabilization of lizardite in preference to chrysotile in the very common mesh serpentine of mantle dunites and harzburgites, unlike that for lizardite in bastites and veins, is not strong. The lizardite of mesh serpentinite is typically relatively Mg-rich, with X_{Mg} in range 0.93 to 0.96, the remainder consisting of Fe^{2+}, Fe^{3+}, Al, Cr, and Ni end-members. For the sake of argument, let us suppose that the hypothetical chrysotile in exchange equilibrium with Liz (X_{Mg} = 0.94) has X_{Mg} = 0.97 (less Al, Cr and Fe^{3+}, more Fe^{2+} and Ni). The equilibrium shift per mole from pure MSH for coexisting lizardite and chrysotile is given reasonably well by: $\delta\Delta G_r = 3RT[\ln X_{Mg}liz - \ln X_{Mg}chr]$, which assumes charge-balanced substitution of R^{3+} cations, as shown to be the case for lizardite by O'Hanley and Dyar (1993). At 200°C we find that lizardite is favored by −371 J/mol. This number is comparable to the molar surface energy of lizardite and is much less than that of chrysotile; it disappears in the "noise" when compared to the strain energy in chrysotile. If ΔS of the transition Liz = Chr is 5 J/K.mol (see estimate below), then the corresponding equilibrium shift is + 74°C. Chrysotile and lizardite at the same site in nature seem to differ in X_{Mg} by less than in the example given here; on the other hand, the entropy change could be smaller and the calculated equilibrium shift larger. While it would be foolish to deny the influence of impurities on the polymorphic equilibrium, its role in the occurrence of Liz vs. Chr in most serpentinites seems to be overshadowed by the mode-of-occurrence factors discussed above. In any case, laboratory evidence in the pure system MSH (see below) indicates that impurity stabilization is not

necessary to drive the Chr-to-Liz reaction in the 200 to 300°C range.

Evidence for the passage in time from predominantly lizardite serpentinite to chrysotile-bearing "recrystallized" serpentinite (in which chrysotile may become pervasive), whatever the cause, is based largely on polarized light microscopy, substantiated in many instances by *in situ* microbeam X-ray diffraction (e.g., Laurent, 1975; Mumpton and Thompson, 1975; Wicks and Plant, 1979; Prichard, 1979; Cogulu and Laurent, 1984; Wicks and O'Hanley, 1988; O'Hanley et al., 1989; O'Hanley, 1991; O'Hanley and Wicks, 1995; O'Hanley, 1996). The change is interpreted directly in terms of the polymorphic reaction. The frequency of descriptions of the Liz-to-Chr transition in serpentinite is impressive. However, there is little microscopic evidence that it is pseudomorphic, and indeed little reason to believe that it should be so. TEM imaging can provide the subtle evidence needed to prove a replacement, as in the case of calcite by chrysotile (Baronnet and Belluso, 2002, Fig. 10) and antigorite by chrysotile (Auzende et al., 2002). The replacement of lizardite by chrysotile has also been seen with the TEM (A. Baronnet, pers. commun., March 2002). In principle, there is no reason why the Liz-to-Chr transition should not take place spontaneously in nature, but the laboratory evidence discussed below suggests that higher temperatures are needed for simple isochemical replacement than are believed the case (≈ 300°C) for many chrysotile localities (O'Hanley and Wicks, 1995; O'Hanley, 1996).

Relative Stability of Chrysotile and Lizardite: Laboratory Evidence

Is it possible that there is a lizardite-to-chrysotile transition up-temperature that takes place metastably in the stability field of antigorite? The few experiments that have been done do not yet provide a conclusive answer, but they suggest that the rate of the polymorphic transition is not impossibly slow in hydrothermal systems using large fluid/mineral ratios, and that carefully designed experiments with well-characterized run products and months-long run times might provide more definitive data.

Chernosky (1975) found that hydrothermal treatment for two to three months at 2 kbar of a starting mix in the system MSH consisting of chrysotile + platy serpentine produced 100% chrysotile at 431°C and 100% platy serpentine (resembling lizardite) at 413°C, as determined by X-ray powder diffraction. Chernosky et al. (1988) revised these temperatures to 438°C and 418°C respectively, and concluded that lizardite has a lower thermal stability than chrysotile at 2 kbar.

In experiments with reactants + products of the hydration reaction of olivine:

$$2 \, Fo + 3 \, H_2O = Serp + Brc \qquad (6)$$

on the bulk composition of olivine Fo_{93} + H_2O at 341°C, 1 kbar (33 days) and 361°C, 2 kbar (24 days), Moody (1976) tentatively concluded from SEM observations that chrysotile had formed during the runs at the expense of lizardite, and that chrysotile is the stable serpentine immediately below the hydration reaction curve. A similar observation was made by Wegner and Ernst (1983) in the MSH system, namely the growth of minor amounts of chrysotile in their longest duration experiments, which otherwise produced lizardite and brucite.

Recent laboratory work in the pure system MSH at lower temperatures using gel starting materials found progress of the polymorphic reaction in the opposite direction. In a study of run products over time using HRTEM and other techniques, Grauby et al. (1998) showed that prolonged (up to 6 months) hydrothermal treatment of an ideal serpentine composition with excess H_2O, at 300°C and 0.7 kbar, resulted in the replacement of first-grown cylindrical and conical chrysotile by polygonal serpentine and then finally lizardite. These observations were interpreted as transitions driven by Ostwald ripening, with chrysotile the kinetically most favored phase and lizardite the most stable. The same result was obtained at 200°C (A. Baronnet, pers. commun., March 2002). These results agree well with the evolution of chrysotile → polygonal serpentine → lizardite microstructures in nature, as viewed by TEM. A further long-duration experiment at 400°C and appropriate pressure would clearly be helpful in the context of a possible reversal of the polymorphic transition. The *rate* of transition from chrysotile to lizardite under favorable conditions in the laboratory is in marked contrast to nature, where chrysotile has survived since Precambrian times (O'Hanley, 1996).

In flow-through experiments on the hydrothermal alteration of olivine at 300°C and 300 bars, Normand et al. (2002) found lizardite to be the dominant serpentine mineral at the inlet of the tubular flow-cell, and chrysotile at the outlet. They interpreted

these results in terms of lizardite crystallization under supersaturated conditions, and chrysotile nucleation on earlier formed lizardite at higher levels of supersaturation. These experiments may be reconciled if we postulate faster nucleation and growth rates for chrysotile from strongly supersaturated fluid (from dissolution of gels and oxides), and faster rates for lizardite at low degrees of supersaturation in the presence of olivine.

A Possible MSH Phase Diagram

We develop here a possible P - T phase diagram by accepting the MSH data of Berman (1988), and adding to them an estimate of the 298K, 1 bar thermodynamic properties of a provisional lizardite based on those of chrysotile. We give lizardite the same second-derivative thermodynamic properties as those of chrysotile. We accept the field and laboratory evidence that lizardite is the lower-temperature, hence lower-entropy phase, and make a guess that at 298 K and 1 bar $S_{liz} = S_{chr} - 5$ (J/K.mol), a difference of 2.5%. For comparison, the reference state entropy of reaction 1 is 2.9 J/K per mol Chr, a difference of 1.3%. The source of the entropy of transition is not obvious from the crystal structures, given that a three-dimensional refinement of chrysotile is not available, but a reasonable inference is that it concerns differences in hydrogen bonding and the extent of ordering between layers (Dódony and Buseck, 2004).

A value of ΔH_f at 298 K and 1 bar for our provisional lizardite (–4,366,856.0, as compared to –4,363,356.0 J/mol for chrysotile) is chosen to make Liz and Chr in equilibrium at 425°C at 2 kbar after Chernosky (1975). In doing this, we should remember that chrysotile may not possess a unique enthalpy of formation, depending on how its standard state is defined in terms of radii, and that the number adopted is an integrated value suggested by the phase equilibrium data. We should also recognize that the critical Chernosky bracket might not be supported by future experiments using phase characterization by TEM. Nevertheless, a substantially more stable lizardite is unlikely: for example, a 1500 J/mol more negative ΔH_f stabilizes lizardite to higher than 400°C and limits the paragenesis Atg + Brc (Peretti et al., 1992) to pressures above 5 kbar (even higher pressures if the fluid is not pure H_2O). This means that in the temperature range 300–400°C lizardite is unlikely to be greater than about 2 kJ more stable than bulk chrysotile.

Identical molar volumes for lizardite and chrysotile are adopted, for the following reasons. The platy serpentine synthesized in MSH by Chernosky (1975, experiment 241M) was reported to have a 0.6% smaller cell volume than chrysotile of the same composition. However, this platy serpentine has an anomalously small cell volume and c dimension in comparison to an extrapolation to zero Al from a series of aluminous lizardites in the same study (Chernosky, 1975, Figs. 2, 3, 5), and the extrapolated volume is within error the same as that of chrysotile. The cell volumes of a series of serpentines produced from olivine by Moody (1976), with unknown and no doubt variable Fe contents, suggest that lizardite might be 0.3% smaller than chrysotile (ignoring outlier data). This may be true, but it seems premature to this writer to assume that lizardite is the denser phase and therefore favored over chrysotile by an increase in pressure (cf. Chernosky et al., 1988; Wicks and O'Hanley, 1988; O'Hanley et al., 1989). It is true that the smaller volume of Liz would be consistent with the usual correlation between the molar entropy and volume of phases.

The phase diagram created by adding lizardite (Fig. 5) is very similar to that of Chernosky et al. (1988) except that the calculated H_2O-conserved reaction 1 is now: 17 Liz = Atg + 3 Br, and is located 65°C higher than was the case for chrysotile. Chrysotile is absent from the phase diagram.

Application of the MSH phase diagram to the mineral parageneses in serpentinites is far from straightforward given that most serpentinitess contain more than one of the common rock-forming serpentine minerals, in microstructural arrangements that in most cases can only be clarified by TEM examination. For other polymorphic mineral groups occurring in crystalline rocks, such as the aluminosilicate minerals, petrologists commonly infer growth of a polymorph as taking place within its P-T stability field, and appeal to sluggish dissolution rates to account for the coexistence of two or three in one rock. This approach needs to be modified for the serpentine minerals crystallizing at low temperature to allow for an Ostwald step process that may fail to reach the most stable form. On higher steps are the less common naturally occurring polytypes of serpentine, maybe carlosturanite and balangeroite, and (by a slim margin) chrysotile. For most of these species, their occurrence has to be related to circumstances attending nucleation and growth, rather than unique combinations of P and T where each one might be stable.
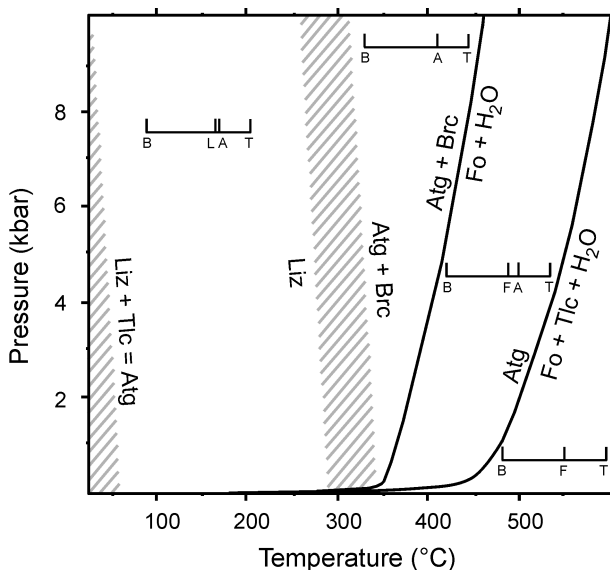
FIG. 5. A possible stable phase diagram for the system MSH. To emphasize the uncertainty in their locations, the two steep H_2O-conserved reactions are shown as shaded areas.

The MSH phase diagram of Figure 5 clearly does not predict the widespread occurrence of chrysotile in nature. In fact, in the 250 to 425°C range, chrysotile is two stability levels removed from the stable assemblage. This is somewhat disconcerting, given that field observations allow us to recognize a class of recrystallized prograde serpentinites (O'Hanley et al., 1989) characterized by the growth of matrix chrysotile from lizardite, together with chrysotile in veins. Recrystallized serpentinites containing chrysotile ± lizardite and antigorite in many instances are believed to have involved temperatures of less than 300°C (O'Hanley, 1996). If our phase diagram is correct, the direct replacement of lizardite by chrysotile should not be possible until the temperature exceeds 425°C; and the case for impurity stabilization of chrysotile is not compelling.

Given the role that appears to be played by kinetics in the growth of the minerals in serpentinites, an isobaric (2 kbar) diagram plotting reaction free energy (driving force for reaction) against temperature (Fig. 6), using the same data as in Figure 5, perhaps offers more insight into the possible occurrences of the MSH minerals than the stable PT-phase diagram. All curves in Figure 6 are relative to the free energy of one mole of bulk chrysotile. With small adjustments (Fig. 6 caption), this dia-

gram works equally well for lizardite as the reactant. Reactions that evolve significant amounts of H_2O have steep slopes, whereas H_2O-conserved reactions are flat. Not taken into account in Figure 6, of course, is the dependence of reaction rates on temperature (Martin and Fyfe, 1970) and effective fluid/rock ratios, and the small effect of Fe on the reaction locations. This diagram shows the following in the case of *progressive metamorphism*.

1. The driving force to form antigorite + brucite from chrysotile or lizardite (the H_2O conserved reaction 1) remains small (< 2 kJ) up to 500°C. No H_2O is released by this reaction to catalyze it. It is very unpromising as a petrologic indicator, and should not be used to constrain the temperature of occurrences of chrysotile or lizardite.

2. An alternative reaction terminal to chrysotile or lizardite is metastable and produces olivine:

$$20 \ Chr/Liz = Atg + 6 \ Fo + 9 \ H_2O. \qquad (7)$$
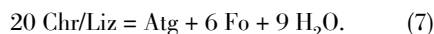
Above 380°C its reaction free energy is larger than reaction 1 (per mol. Chr); moreover, H_2O is released, so it is a more promising reaction for the decomposition of Chr/Liz in nature. Reaction 7 was inferred by Peretti et al. (1992) to account for the first occurrence of olivine in the progressive metamorphism of the Malenco serpentinite, Italy.
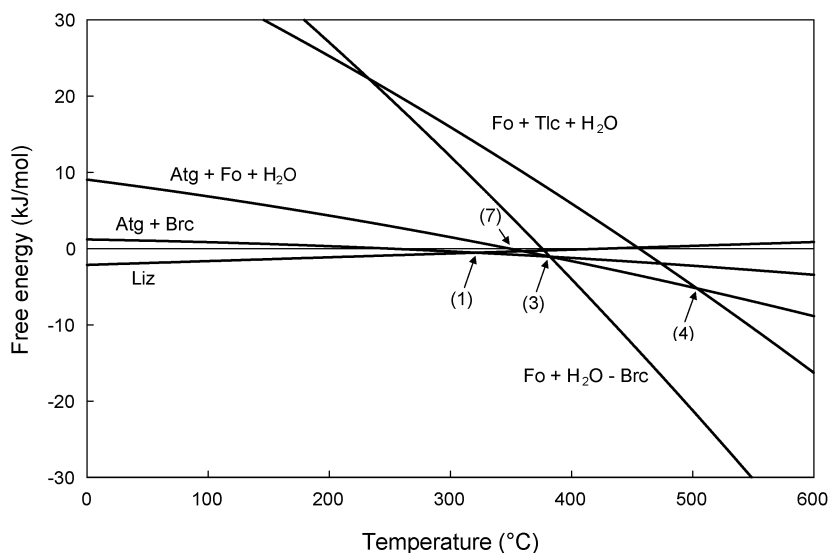
Fig. 6. Free energy at 2 kbar for reactions in the system MSH from one mole of bulk chrysotile (cf. Fig. 1) to the compositional equivalents indicated. Temperatures of stable reactions 1, 3, and 4 (Fig. 5), and metastable reaction 7, are shown by arrows. To convert to lizardite as reactant: subtract from the curves the small ΔG of Chr $\rightarrow$ Liz (i.e., rotate the curves clockwise about T = 425°C), and reflect the curve labeled Liz across the $\Delta G = 0$ line to become curve Chr.

3. The traditional olivine-in reaction (3 for reactant Atg, 6 for metastable reactants Liz/Chr) applies only to brucite-bearing serpentinites. This means metadunites, assuming that they have not at some stage absorbed SiO_2. That this tends to happen is suggested by the general decline in modal brucite as recrystallization of serpentinite progresses (O'Hanley and Dyar, 1993), the absence of brucite where it might be expected (Coleman, 1971), whole-rock compositional changes (Condie and Madison, 1969), and mass-balance studies like those of Labotka and Albee (1979). Only 10°C separates reactions 6 and 3. Reaction 6 was inferred by Pinsent and Hurst (1977), and reaction 3 by Peretti et al. (1992), who found it to be upgrade from reaction 7. There will be cases where it might be difficult to distinguish the effect of progress of reaction 6 from reaction 7. The modal amount of olivine produced by reactions 6 and 7 will not be large: no more than 13% in 7 and a similar amount in 6, depending on the amount of brucite.

4. Where chrysotile might be able to form from lizardite (>425°C?), it is already less stable than antigorite + olivine + H_2O (reaction 7) by more than 3 kJ. If the diagram is appropriate and correct, most chrysotile formation in nature has taken place metastably with respect to lizardite.

5. The drive to form antigorite-bearing assemblages from chrysotile or lizardite, whether by reaction 1 or reaction 7, remains small ($\Delta G < 5$ kJ) even as high as 500°C. Dungan (1977) and Viti and Mellini (1998) attributed the breakdown of lizardite + chrysotile directly to forsterite (+ talc?) rather than to antigorite to the rapid rate of temperature increase attending contact metamorphsim, and the sluggish growth kinetics of antigorite. Relics of chrysotile were found by Mellini et al. (1987) in the Malenco serpentinite to survive well into the zone of antigorite (435°C according to calcite-dolomite thermometry).

6. Above 500°C the drive to form olivine + talc (reaction 4) quickly overtakes the other reactions.

Figure 6 shows that by *retrograde metamorphism* below 460°C at 2 kbar, any of antigorite, lizardite, and chrysotile could in theory form following introduction of H_2O into a metaperidotite composed of olivine ± talc, anthophyllite, or enstatite. Down to about ~ 310°C we believe the most stable serpentine is antigorite (with brucite or talc, Fig. 5). At 300°C the free energy lost by serpentinization of peridotite is more than 10 kJ/mol Srp., whereas lizardite, chrysotile, and antigorite (+ Brc) themselves differ in free energy by less than 1 kJ. Classical thermodynamics cannot tell us which one will form.

However, in nature, as discussed earlier, the rate of introduction of H_2O to the site of reaction in a partially serpentinized peridotite may be so slow that $a(H_2O)$ becomes rock-buffered (Ol + Brc + Serp) to low values: fluid-absent conditions, or H_2O dissolved in other gas species. Figure 6 then becomes inappropriate; fluid buffering reduces the free energy drive for hydration to zero (for example, when $a(H_2O) = 0.1$ and T = 200°C, $3RT\ln a(H_2O)$ = –27 kJ; cf. Fig. 6). Under these circumstances, it is possible that only the most stable serpentine will form, namely lizardite, and the system might discriminate against less stable serpentines. Should fluid-buffering conditions be interrupted by a major inflow of H_2O, made possible perhaps by tectonic movements, the large energy drive for serpentinization (Fig. 6) will be restored. This could account for the more diverse assemblage of serpentine minerals commonly found in mesh cores. Viti and Mellini (1998) proposed exactly this scenario: mesh rims form by a thermodynamically controlled reaction; mesh cores form by a kinetically controlled reaction in an environment of local fluid supersaturation. An hourglass structure signifies the absence of this fluid influx and a continuation of buffered lizardite growth to the exhaustion of olivine.

Figure 6 refers to the composition of ideal serpentine, and for systems with more or less Mg/Si we must consult Figure 5. For bastite after orthopyroxene, Figure 5 (and earlier published phase diagrams) predicts the local assemblage Atg + Tlc rather than Liz + Tlc, although the latter is much more common. We can invoke stabilization of lizardite perhaps by the large amounts of R^{3+} present, or alternatively cite the ease with which lizardite can nucleate on orthopyroxene. With its layer curvature, antigorite may have growth requirements that are not unlike those of chrysotile.

The precipitation of chrysotile from ground water at or close to the Earth's surface (e.g., Peters, 1993) can be attributed to supersaturation resulting from the metastable equilibrium dissolution of residual forsterite or enstatite (Nesbitt and Bricker, 1978). At very low temperatures, the serpentinization reactions are sluggish in comparison to dissolution rates. Chrysotile forms rather than the more stable lizardite for the same kinetic reasons discussed earlier for chrysotile in veins.

The difference in the molar free energies of average or bulk chrysotile and lizardite in the 300 to 500°C range is shown in Figure 6 to be as small as 300 J/mol or less. If these numbers are correct, experimental phase equilibrium brackets for the dehydration reactions of chrysotile and lizardite should be indistinguishable. Our model reaction free energies for the Liz = Chr reaction are small in comparison to possible molar energy differences attributable to strain, defects, surface energies, and polytypism of these minerals in nature. Figure 6 offers very little if any guidance to the occurrence of lizardite vis-à-vis chrysotile in nature. Unless there are problems with our interpretation of the experimental data, bulk chrysotile has no field of stability of its own in the system MSH. Lizardite is the stable low-temperature form of serpentine and antigorite the high temperature form. Good parallels are provided by the analogous system Al_2O_3–SiO_2–H_2O, in which the low-temperature minerals dickite and halloysite (and nacrite) are less stable than kaolinite (Anovitz et al., 1991).

Concluding Remarks

The relative distribution of chrysotile and lizardite in serpentinites and magnesian marbles can be understood not in terms of the temperature and pressure of their crystallization, but according to their modes of formation. Lizardite replaces olivine and other peridotite minerals during hydration in microenvironments of small porosity and low permeability where part of the enthalpy released by reaction is converted into PdV work related to lizardite's force of crystallization. This effort is possibly reflected in the mesh and hourglass texture after olivine where (001) of lizardite is oriented normal to the expansion stress, and perhaps also in the α-serpentine habit of the apparent fibers. Chrysotile finds it difficult to nucleate and grow in nature from olivine during hydration, but instead crystallizes in cracks and other voids that develop mostly after hydration is complete. These two contrasting environments may be in close proximity as, for example, in the rims and cores of kernel structure, such that chrysotile and lizardite grow simultaneously under the same conditions of temperature and pressure. Table 2 provides suggestions with regard to the conditions accompanying the three serpentine minerals in nature.

Laboratory investigations indicate that lizardite is more stable in the MSH system than chrysotile with "average" thermodynamic properties up to ~400°C or higher, which is inside the stability field of antigorite. Despite an up-temperature transition from lizardite to chrysotile at these temperatures,

TABLE 2. Generalized Conditions for Serpentine Formation

	Lizardite	Chrysotile	Antigorite
Approximate temp. (°C)	50–300	0–400	250–600
P_{H2O}/P_{lith}	<1	~1	~1
W/R ratio	small	large	small
Fluid supersaturation	low	low-high?	low
Shear stress?	stable	unstable	stable
Principal mode of origin	Hydration of peridotite	Veins and replacements	Recryst. of serp. Hydrat. of peridotite

the latter remains metastable. Growth of cross- and slip-fiber chrysotile in veins in lizardite- and antigorite-bearing serpentinite, and as apparent replacements of these minerals, may be explained by the presence of mildly supersaturated fluid, and the opportunity to nucleate chrysotile cylinders with low-strain, and possibly stable, nucleii, thereby favoring further growth of chrysotile. The dynamic tectonic environments typical of asbestos deposits promote the development of cracks, but chrysotile itself grows under isotropic stress while bathed in hydrous fluid. The contrasting behaviors of lizardite and chrysotile correspond to what have in the past been called a stress-antistress mineral pair. The persistence and even growth of chrysotile and lizardite in the stability field of antigorite is made possible by the sluggish growth kinetics of the antigorite.

Insufficient data are available for a realistic evaluation of equilibrium displacement of lizardite versus chrysotile caused by the presence of components outside the system MSH. Except when lizardite is distinctly aluminous, the energetic shifts seem likely to be smaller than energy uncertainties related to grain boundaries, crystal defects, polytypism, and especially the radius-dependent elastic strain in chrysotile.

Could chrysotile actually possess a stability field if we had more accurate data? Two constraints would need to be relaxed: (1) the calculated temperature of reaction 1 for chrysotile (Chernosky et al., 1988), which has a large uncertainty, would need to be at least 100°C higher; and (2) rather than near or above 400°C, the lizardite to chrysotile transition would need to be ~300°C. In both cases, the essence of the problem is the unambiguous characterization of run products in laboratory experiments, especially for

the H_2O-conserved reactions, as in the work of Grauby et al. (1998). The experimental brackets used for the thermodynamic database have relied on relative peak heights in X-ray diffractograms; unfortunately, in complex powder mixtures, XRD cannot always provide the resolution among the serpentine polymorphs that is needed. In future experimental work, we must find some way to recognize the consequences of the effect of P and T on the composition and molar free energy of polysomatic antigorite, and the influence of different populations of chrysotile cylinder radii on its thermodynamic properties. There may be some merit in further solubility studies in the MSH system, and a calorimetric study might profitably be made of chrysotile synthesized (if possible) with different radii. Most important of all is further TEM characterization of the microstructures and reaction relations of minerals in natural serpentinites.

REFERENCES

Abrajano, T. A., Sturchio, N. C., Bohlke, J. K., Lyon, G. L., Poreda, R. J., and Stevens, C. M., 1988, Methane-hydrogen gas seeps, Zambales ophiolites, Philippines: Deep or shallow origin?: Chemical Geology, v. 71, p. 211–222.

Abrajano, T. A., Sturchio, N. C., Kennedy, B. M., Lyon, G. L., Muehlenbachs, K., and Bohlke, J. K., 1990, Geochemistry of reduced gas related to serpentinization of the Zambales ophiolites, Philippines: Applied Geochemistry, v. 5, p. 625–630.

Anovitz, L. M., Perkins, D., and Essene, E. J., 1991, Metastability in near-surface rocks of minerals in the system Al_2O_3–SiO_2–H_2O: Clays and Clay Minerals, v. 39, p. 225–233.

Auzende, A., Devouard, B., Guillot, S., Daniel, I., Baronnet, A., and Lardeaux, J., 2002, Serpentinites from Central Cuba, a petrology and HRTEM study: European Journal of Mineralogy, v. 14, p. 905–914.

Bain, G. W., 1932, Chrysotile asbestos: II. Chrysotile solutions: Economic Geology, v. 27, p. 281–296.

Banfield, J. F., Bailey, S. W., Barker, W. W., and Smith, R. C., 1995, Complex polytypism: Relationships between serpentine structural characteristics and deformation: American Mineralogist, v. 80, p. 1116–1131.

Barnes, I., O'Neil, J. R., and Trescades, J. J., 1978, Present day serpentinization in New Caledonia, Oman and Yugoslavia: Geochimica et Cosmochimica Acta, v. 42, p. 144–145.

Barnes, I., Rapp, J. B., O'Neil, J. R., Sheppard, R. A., and Gude, A. J., 1972, Metamorphic assemblages and the direction of fluid flow in four instances of serpentinization: Contributions to Mineralogy and Petrology, v. 35, p. 263–276.

Baronnet, A., and Boudier, F., 2001, Microstructural and microchemical aspects of serpentinization [abs.]: Seventh Annual V. M. Goldschmidt Conference, Abstracts.

Baronnet, A., and Belluso, E., 2002, Microstructures of the silicates: Key information about mineral reactions and a link with the Earth and materials sciences: Mineralogical Magazine, v. 66, p. 709–732.

Baronnet, A., and Devouard, B., 1996, Topology and crystal growth of natural chrysotile and polygonal serpentine: Journal of Crystal Growth, v. 166, p. 952–960.

Baronnet, A., Mellini, M., and Devouard, B., 1994, Sectors in polygonal serpentine. A model based on dislocations: Physics and Chemistry of Minerals, v. 21, p. 330–343.

Belluso, E., and Ferraris, G., 1991, New data on balangeroite and carlosturanite from alpine serpentinite: European Journal of Mineralogy, v. 3, p. 559–566.

Berman, R. G., 1988, Internally consistent thermodynamic data for stoichiometric minerals in the system Na_2O-K_2O-CaO-MgO-FeO-Al_2O_3-SiO_2-TiO_2-H_2O-CO_2: Journal of Petrology, v. 29, p. 445–522.

Berman, R. G., Engi, M., Greenwood, H. J., and Brown, T. H., 1986, Derivation of internally consistent thermodynamic data by the technique of mathematical programming; a review with application to the system MgO-SiO_2-H_2O: Journal of Petrology, v. 27, p. 1331–1364.

Bernt, M. E., Allen, D. E., and Seyfried, W. E., 1996, Reduction of CO_2 during serpentinization of olivine at 300°C and 500 bar: Geology, v. 24, p. 351–354.

Bloss, F. D., 1994, Crystallography and crystal chemistry: Washington DC, Mineralogical Society of America, 545 p.

Bogolepov, V. G., 1970, Problem of serpentinization of ultrabasic rocks: International Geology Review, v. 12, p. 421–432.

Bons, P. D., and Jessell, M. W., 1997, Experimental simulation of fibrous veins by localised dissolution-precipitation creep: Mineralogical Magazine, v. 61, p. 53–63.

Bostock, B. C., Hyndman, R. D., Rondenay, S., and Peacock, S. M., 2002, An inverted continental Moho and the serpentinization of the forearc mantle: Nature, v. 417, p. 536–538.

Bowen, N. L., and Tuttle, O. F., 1949, The system MgO-SiO_2-H_2O: Geological Society of America Bulletin, v. 80, p. 1947–1960.

Brearley, A. J., and Jones, R. H., 1997, Chondritic meteorites, *in* Papike, J. J., ed., Planetary materials: Reviews in Mineralogy, v. 36, p. 3-1 to 3-398.

Brocher, T. M., Parsons, T., Tréhu, A. M., Snelson, C. M., and Fisher, M. A., 2003, Seismic evidence for widespread serpentinized forearc upper mantle along the Cascadia Margin: Geology, v. 31, p. 267–270.

Bromiley, G. D., and Pawley, A. R., 2003, The stability of antigorite in the systems MgO–SiO_2–H_2O (MSH) and MgO–Al_2O_3–SiO_2–H_2O (MASH): The effects of Al^{3+} substitution on high-pressure stability: American Mineralogist, v. 88, p. 99–108.

Brown, E. H., Wilson, D. L., Armstrong, R. L., and Harakal, J. E., 1982, Petrologic, structural, and age relations of serpentinite, amphibolite, and blueschist in the Shuksan Suite of the Iron Mountain–Gee Point area, North Cascades, Washington: Geological Society of America Bulletin, v. 93, p. 1087–1098.

Burkhard, D. J. M., and O'Neil, J. R., 1988, Contrasting serpentinizing processes in the eastern Central Alps: Contributions to Mineralogy and Petrology, v. 99, p. 498–506.

Caruso, L. J., and Chernosky, J. V., Jr., 1979, The stability of lizardite: Canadian Mineralogist, v. 17, p. 757–770.

Cashman, S. M., and Whetten, J. T., 1976, Low-temperature serpentinization of peridotite fanglomerate on the west margin of the Chiwaukum graben, Washington: Geological Society of America Bulletin, v. 87, p. 1773–1776.

Chernosky, J. V., Jr., 1975, Aggregate refractive indices and unit cell parameters of synthetic serpentine in the system MgO–Al_2O_3–SiO_2H_2O: American Mineralogist, v. 60, p. 200–208.

———, 1982, The stability of clinochrysotile: Canadian Mineralogist, v. 20, p. 19–27.

Chernosky, J. V., Jr., Berman, R. G., and Bryndzia, L. T., 1988, Serpentine and chlorite equilibria, *in* Bailey, S. W., ed., Hydrous phyllosilicates other than micas:

Insights from eastern Ladakh, northwest Himalayas: Geology, v. 28, p. 199–202.

Guggenheim, S., and Eggleton, R. A., 1988, Crystal chemistry, classification, and identification of modulated layer silicates, *in* Hydrous phyllosilicates (exclusive of micas): Reviews in Mineralogy, v. 19, Mineralogical Society of America, p. 675–725.

Hacker, B. R., and Peacock, S. M., 1995, Creation, observation, and exhumation of UHPM rocks, *in* Coleman, R. G., and Wang, X., eds., Ultrahigh pressure metamorphism: Cambridge, UK, Cambridge University Press, p. 159–181.

Hatch, F. H., Wells, A. K. and Wells, M. K., 1949, The petrology of the igneous rocks: London, UK, Thomas Murby and Co., 469 p.

Helgeson, H. J., Delaney, J. M., Nesbitt, H. W., and Bird, D. K., 1978, Summary and critique of the thermodynamic properties of rock-forming minerals: American Journal of Science, v. 278-A, p. 1–229.

Hemley, J. J., Montoya, J. W., Christ, C. L., and Hostetler, P. B., 1977, Mineral equilibria in the $MgO–SiO_2–H_2O$ system. I. Talc-chrysotile-brucite stability relations: American Journal of Science, v. 277, p. 322–351.

Hostetler, P. B., Coleman, R. G., Mumpton, F. A., and Evans, B. W., 1966, Brucite in alpine serpentinites: American Mineralogist, v. 51, p. 75–98.

Igarashi, T., Katoh, T., and Niida, K., 1985, The Takadomari serpentinites in the Kamuikota ophiolites belt, Hokkaido, Japan: Journal of the Faculty of Science, Hokkaido University, Series IV, v. 21, p. 305–319.

Iishi, K., and Saito, M., 1973, Synthesis of antigorite: American Mineralogist, v. 58, p. 915–919.

Ikin, N. P., and Harmon, R. S., 1983, A stable isotope study of serpentinization and metamorphism in the Highland border suite, U.K.: Geochimica et Cosmochimica Acta, v. 47, p. 153–167.

Jahns, R. H., 1967, Serpentinites of the Roxbury district, Vermont, *in* Wyllie, P. J., ed., Ultramafic and related rocks: New York, NY, John Wiley and Sons, Inc., p. 137–160.

Johannes, W., 1968, Experimental investigation of the reaction forsterite + H_2O = serpentine + brucite: Contributions to Mineralogy and Petrology, v. 19, p. 309–315.

Kalinin, D. V., and Zubkov, M. Y., 1981, Kinetic investigation of the $MgO–SiO_2–H_2O$ system, reaction: Serpentine = forsterite + talc + water: Soviet Geology and Geophysics, v. 22, no. 9, p. 61–68.

Kelley, D. S., Karson, J. A., Blackman, D. K., Früh-Green, G. L., Butterfield, D. A., Lilley, M. D., Olson, E. J., Schrenk, M. O., Roe, K. K., Lebon, G. T., Rivizzigio, P., and the AT3-60 Shipboard Party, 2001, An off-axis hydrothermal vent field near the Mid-Atlantic Ridge at 30°N: Nature, v. 412, p. 145–149.

Kerrick, D. M., 1990, The fibrolite problem, *in* Kerrick, D. M., ed., The Al_2SiO_5 polymorphs: Reviews in Mineralogy, v. 22, p. 207–222.

Khodyrev, O. Y., and Agoshkov, V. M., 1986, Phase transitions in serpentine in the system $MgO–SiO_2–H_2O$ system at 40–80 kbar: Geochemistry International, v. 23, no. 7, 47–52.

King, E.G., Barany, R., Weller, W. W., and Pankratz, L. B., 1967, Thermodynamic properties of forsterite and serpentine: U.S. Bureau of Mines, Report of Investigations 6962, 19 p.

Korytkova, E. N., and Makarova, L. A., 1972, Experimental investigation of the hydrothermal alteration of olivine in connection with the formation of asbestos: Geochemistry International, v. 9, p. 957–961.

Kunze, G., 1961, Antigorit strukturtheoretische Grundlagen und ihre praktische Bedeutung für die weitere Serpentin-forschung: Fortschritte in Mineralogie, v. 39, p. 206–324.

Labotka, T. C., and Albee, A. L., 1979, Serpentinization of the Belvidere Mountain ultramafic body, Vermont: Mass balance and reaction at the metasomatic front: Canadian Mineralogist, v. 17, p. 831–845.

Laurent, R., 1975, Petrology of the alpine-type serpentinites of Asbestos and Thetford mines, Quebec: Schweizerische Mineralogische und Petrographische Mitteilungen, v. 5, p. 431–455.

Laurent, R., and Hébert, Y., 1979, Paragenesis of serpentine assemblages in harzburgite tectonite and dunite cumulate from the Quebec Appalachians: Canadian Mineralogist, v. 17, p. 857–870.

Le Glueher, M., Livi, K. J. T., Veblen, D. R., Noack, Y., and Amouric, M., 1990, Serpentinization of enstatite from Pernes, France: Reaction microstructures and the role of system openness: American Mineralogist, v. 75, p. 813–824.

Livi, K. J. T., and Veblen, D. R., 1987, "Eastonite" from Easton, Pennsylvania: A mixture of phlogopite and a new form of serpentine: American Mineralogist, v. 72, p. 113–125.

Lowell, R. P., and Rona, P. A., 2002, Seafloor hydrothermal systems driven by the serpentinization of peridotite: Geophysical Research Letters, v. 29, p. 11 [10.1029/2001GLO14411].

MacDonald, A. H., and Fyfe, W. S., 1985, Rates of serpentinization in seafloor environments: Tectonophysics, v. 116, p. 123–135.

Majzlan, J., Navrotsky, A., and Casey, W. H., 2000, Surface enthalpy of boehmite: Clays and Clay Minerals, v. 48, p. 699–707.

Maltman, A. J., 1978, Serpentinite textures in Anglesey, North Wales, United Kingdom: Geological Society of America Bulletin, v. 89, p. 972–980.

Martin, B., and Fyfe, W. S., 1970, Some experimental and theoretical observations on the kinetics of hydration reactions with particular reference to serpentinization: Chemical Geology, v. 6, p. 185–202.

Means, W. D., 1987, A newly recognized type of slickenside striation: Journal of Structural Geology, v. 9, p. 585–590.

Mellini, M., 1982, The crystal structure of lizardite-1T: Hydrogen bonds and polytypism: American Mineralogist, v. 67, p. 587–598.

———, 1986, Chrysotile and polygonal serpentine from the Balangero serpentinite: Mineralogical Magazine, v. 50, p. 301–306.

Mellini, M., Ferraris, G., and Compagnoni, R., 1985, Carlosturanite: HRTEM evidence of a polysomatic series including serpentine: American Mineralogist, v. 70, p. 773–781.

Mellini, M., Trommsdorff, V., and Compagnoni, R., 1987, Antigorite polysomatism: Behaviour during progressive metamorphism: Contributions to Mineralogy and Petrology, v. 97, p. 147–155.

Mellini, M., and Viti, C., 1994, Crystal structure of lizardite-1T from Elba, Italy: American Mineralogist, v. 79, p. 1194–1198.

Mellini, M., and Zanazzi, P. F., 1987, Crystal structures of lizardite-$1T$ and lizardite-$2H_1$ from Coli, Italy: American Mineralogist, v. 72, p. 943–948.

Mellini, M., and Zussman, J., 1986, Carlosturanite (not "picrolite") from Taberg, Sweden: Mineralogical Magazine, v. 50, p. 675–679.

Merino, E., and Dewers, T., 1998, Implications of replacement for reaction-transport modeling: Journal of Hydrology, v. 209, p. 137–146.

Mitchell, R. H., and Putnis, A., 1988, Polygonal serpentine in segregation–textured kimberlites: Canadian Mineralogist, v. 26, p. 991–997.

Moody, J. B., 1976, An experimental study on the serpentinization of iron-bearing olivines: Canadian Mineralogist, v. 14, p. 462–478.

Mumpton, F. A., and Thompson, C. S., 1975, Mineralogy and origin of the Coalinga asbestos deposit: Clays and Clay Minerals, v. 23, p. 131–143.

Nagy, B., and Faust, G. T., 1956, Serpentines: Natural mixtures of chrysotile and antigorite: American Mineralogist, v. 41, p. 817–838.

Neal, C., and Stanger, G., 1983, Hydrogen generation from mantle source rocks in Oman: Earth and Planetary Science Letters, v. 66, p. 315–320.

Nesbitt, H. W., and Bricker, O. P., 1978, Low temperature alteration processes affecting ultramafic bodies: Geochimica et Cosmochimica Acta, v. 42, p. 403–410.

Noll, W., 1950, Synthesen im System $MgO/SiO_2/H_2O$: Zeitschrift fuer Anorganische Chemie, v. 261, p. 1–25.

Normand, C., Williams-Jones, A. E., Martin, R. F., and Vali, H., 2002, Hydrothermal alteration of olivine in a flow-through autoclave: Nucleation and growth of serpentine phases: American Mineralogist, v. 87, p. 1699–1709.

Nosaka, T., 2003, Compositional heterogeneity of olivine in thermally metamorphosed serpentinite from southwest Japan: American Mineralogist, v. 88, p. 1377–1397.

O'Hanley, D.S., 1987, The origin of chrysotile asbestos veins in southeastern Quebec: Canadian Journal of Earth Sciences, v. 24, p. 1–9.

———, 1988, The origin of alpine peridotite hosted, cross fiber, asbestos deposits: Economic Geology, v. 83, p. 256–265.

———, 1991, Fault-related phenomena associated with hydration and serpentine recrystallization during serpentinization: Canadian Mineralogist, v. 29, p. 21–35.

———, 1992, Solution to the volume problem in serpentinization: Geology, v. 20, p. 705–708.

———, 1996, Serpentinites: Records of tectonic and petrologic history: Oxford, UK, Oxford University Press, 277 p.

O'Hanley, D. S., Chernosky, J. V., Jr., and Wicks, J. F., 1989, The stability of lizardite and chrysotile: Canadian Mineralogist, v. 27, p. 483–494.

O'Hanley, D.S., and Dyar, M. D., 1993, The composition of lizardite $1T$ and the formation of magnetite in serpentinites: American Mineralogist, v. 78, p. 391–404.

———, 1998, The composition of chrysotile and its relation with lizardite: Canadian Mineralogist, v. 36, p. 727–740.

O'Hanley, D. S., and Offler, R., 1992, Characterization of multiple serpentinization, Woodsreef, New South Wales: Canadian Mineralogist, v. 30, p. 1113–1126.

O'Hanley, D. S., and Wicks, J. F., 1995, Conditions of formation of lizardite, chrysotile, and antigorite, Cassiar, British Columbia: Canadian Mineralogist, v. 33, p. 753–774.

Page, N. J., 1966, Mineralogy and chemistry of the serpentine group minerals: Unpubl. Ph.D. thesis, University of California, Berkeley.

———, 1968, Chemical differences among the serpentine "polymorphs": American Mineralogist, v. 53, p. 201–215.

Pasteris, J. D., 1981, Occurrence of graphite in serpentinized olivines in kimberlite: Geology, v. 9, p. 356–359.

Peacock, S., 1987, Serpentinization and infiltration metasomatism in the Trinity peridotite, Klamath province, northern California: Implications for subduction zones: Contributions to Mineralogy and Petrology, v. 95, p. 55–70.

———, 1993, Large-scale hydration of the lithosphere above subducting slabs: Chemical Geology, v. 108, p. 49–59.

Peretti, A., Dubessy, J., Mullis, J., Frost, B. R., and Trommsdorff, V., 1992, Highly reducing conditions during Alpine metamorphism of the Malenco peridotite (Sondrio, northern Italy) indicated by mineral paragenesis and H_2 in fluid inclusions: Contributions to Mineralogy and Petrology, v. 112, p. 329–340.

Peters, E. K., 1993, $\delta^{18}O$-enriched waters of the Coast Range mountains, northern California: Connate and ore-forming fluids: Geochimica et Cosmochimica Acta, v. 57, p. 1093–1104.

Pinsent, R. H., and Hurst, D. M., 1977, The metamorphism of the Blue River ultramafic body, Cassiar, British Columbia, Canada: Journal of Petrology, v. 18, p. 567–594.

Pistorius, C. W. F. T., 1963, Some phase relations in the system MgO–SiO$_2$–H$_2$O to high pressures and temperatures: Neues Jahrbuch für Mineralogie, Monatshefte, v. 11, p. 283–293.

Post, J. L., and Borer, L., 2000, High-resolution infrared spectra, physical properties, and micromorphology of serpentines: Applied Clay Science, v. 16, p. 73–85.

Prichard, H. M., 1979, A petrographic study of the process of serpentinization in ophiolites and the ocean crust: Contributions to Mineralogy and Petrology, v. 68, p. 231–241.

Puschnig, A. R., 2002, Metasomatic alterations at mafic-ultramafic contacts in Valmalenco (Rhetic Alps, N. Italy): Schweizerische Mineralogische und Petrographische Mitteilungen, v. 82, p. 515–536.

Putnis, A., 2002, Mineral replacement reactions: From macroscopic observations to microscopic mechanisms: Mineralogical Magazine, v. 66, p. 689–708.

Ramsay, J. G., and Huber, M. I., 1983, The techniques of modern structural geology. Volume I, strain analysis: London, UK, Academic Press, 307 p.

Rossetti, P., and Zucchetti, S., 1988, Occurrence of native iron, Fe-Co, and Ni-Fe alloys in the serpentinite from the Balangero asbestos mine (Western Italian Alps): Ofioliti, v. 13, p. 43–56.

Roy, D. M., and Roy, R., 1954, An experimental study of the formation and properties of synthetic serpentines and related layer silicate minerals: American Mineralogist, v. 39, p. 957–975.

Sanford, R.F., 1981, Mineralogical and chemical effects of hydration reactions and applications to serpentinization: American Mineralogist, v. 66, p. 290–297.

Schroeder, T., John, B., and Frost, B. R., 2002, Geologic implications of seawater circulation through peridotite exposed at slow-spreading mid-ocean ridges: Geology, v. 30, p. 367–370.

Skarpelis, N., and Dabitzias, S., 1987, The chrysotile asbestos deposit at Zidani, northern Greece: Ofioliti, v. 12, p. 403–410.

Springer, R. K., 1974, Contact metamorphosed ultramafic rocks in the western Sierra Nevada foothills, California: Journal of Petrology, v. 15, p. 160–195.

Thayer, T. P., 1966, Serpentinization considered as a constant-volume process: American Mineralogist, v. 51, p. 685–710.

Toft, P. B., Arkani-Hamed, J., and Haggerty, S. E., 1990, Petrophysics of retrograde serpentinization. Physics of the Earth and Planetary Interiors, v. 65, p. 137–157.

Trommsdorff, V., 1983, Metamorphose magnesiumreicher Gesteine: Kritischer Vergleich von Natur, Experiment und thermodynamischer Datenbasis: Fortschritte in Mineralogie, v. 61, p. 283–308.

Trommsdorff, V., and Evans, B.W., 1972, Progressive metamorphism of antigorite schist in the Bergell tonalite aureole (Italy): American Journal of Science, v. 272, p. 423–437.

Trommsdorff, V., Lopez Sanchez-Vizcaino, V., Gomez-Pugnaire, M. T., and Müntener, O., 1998, High-pressure breakdown of antigorite to spinifex-textured olivine and orthopyroxene, S.E. Spain: Contributions to Mineralogy and Petrology, v. 132, p. 139–148.

Uehara, S., and Shirozu, H., 1985, Variations in chemical composition and structural properties of antigorites: Mineralogical Magazine, v. 12, p. 299–318.

Ueno, T., Furuta, Y., Koyama, T., and Imada, T., 1991, Phase relation among serpentine, brucite and forsterite from 200 to 500 atm water pressure: Mineralogical Journal, v. 15, p. 276–281.

Ulmer, P., and Trommsdorff, V., 1995, Serpentine stability to mantle depths and subduction related magmatism: Science, v. 268, p. 858–861.

Van der Molen, I., and Roermund, H. L. M., 1986, The pressure path of solid inclusions in minerals: The retention of coesite inclusions during uplift: Lithos, v. 19, p. 317–324.

Vance, J. A., and Dungan, M. A., 1977, Formation of peridotites by deserpentinization in the Darrington and Sultan areas, Cscade Mountains, Washington: Bulletin of the Geological Society of America, v. 88, p. 1497–1508.

Veblen, D. R., 1980, Anthophyllite asbestos: Microstructures, intergrown sheet silicates, and mechanism of fiber formation: American Mineralogist, v. 65, p. 1075–1086.

Veblen, D. R., and Buseck, P. R., 1979, Serpentine minerals: Intergrowths and new combination structures: Science, v. 206, p. 1398–1400.

———, 1981, Hydrous pyriboles and sheet silicates in pyroxenes and uralites: Intergrowth microstructures and reaction mechanisms: American Mineralogist, v. 66, p. 1107–1134.

Viti, C., and Mellini, M., 1997, Contrasting chemical compositions in associated lizardite and chrysotile in veins from Elba, Italy: European Journal of Mineralogy, v. 9, p. 585–596.

———, 1998, Mesh textures and bastites in the Elba retrograde serpentinites: European Journal of Mineralogy, v. 10, p. 1341–1359.

Wegner, W. W., and Ernst, W. G., 1983, Experimentally determined hydration and dehydration reactions in the system MgO–SiO$_2$–H$_2$O: American Journal of Science (Orville volume), v. 283-A, p. 151–180.

Wenner, D. B., and Taylor, H. P., 1971, Temperatures of serpentinization of ultramafic rocks based on O^{18}/O^{16} fractionation between coexisting serpentine and magnetite. Contributions to Mineralogy and Petrology, v. 32, p. 165–185.

Whittaker, E. J. W., 1957, The structure of chrysotile. V. Diffuse reflections and the fibre texture: Acta Crystallographica, v. 10, p. 149–156.

Whittaker, E. J. W., and Wicks, F. J., 1970, Chemical differences among the serpentine "polymorphs": A discussion: American Mineralogist, v. 55, p. 1025–1047.

Whittaker, E. J. W., and Zussman, J., 1956, The characterization of serpentine minerals by X-ray diffraction: Mineralogical Magazine, v. 31, p. 106–126.

Wicks, F. J., 1984a, Deformation histories as recorded by serpentinites. I. Deformation prior to serpentinization: Canadian Mineralogist, v. 22, p. 185–195.

———, 1984b, Deformation histories as recorded by serpentinites. II. Deformation during and after serpentinization: Canadian Mineralogist, v. 22, p. 197–203.

———, 1986, Lizardite and its parent enstatite: A study by X-ray diffraction and transmission electron microscopy: Canadian Mineralogist, v. 24, p. 775–788.

———, 2000, Status of the reference X-ray powder-diffraction patterns for the serpentine minerals in the PDF database: Powder Diffraction, v. 15, p. 42–50.

Wicks, F. J., and O'Hanley, D. S., 1988, Serpentine minerals: Structures and petrology, *in* Bailey, S. W., ed., Hydrous phyllosilicates other than micas: Mineralogical Society of America, Reviews in Mineralogy, v. 19, p. 295–346.

Wicks, F. J., and Plant, A. G., 1979, Electron-microprobe and X-ray-microbeam studies of serpentine textures: Canadian Mineralogist, v. 17, p. 785–830.

Wicks, F. J., and Whittaker, E. J. W., 1975, A reappraisal of the structures of the serpentine minerals: Canadian Mineralogist, v. 13, p. 227–243.

———, 1977, Serpentine textures and serpentinization: Canadian Mineralogist, v. 15, p. 459–488.

Wicks, F. J., Whittaker, E. J. W., and Zussman, J., 1977, An idealised model for serpentine textures after olivine: Canadian Mineralogist, v. 15, p. 446–458.

Williams-Jones, A. E., Normand, C., Clark, J. R., Vali, H., and Martin, R. F., 2001, Controls of amphibole forma-

tion in chrysotile from the Jeffrey Mine, Asbestos, Quebec: Canadian Mineralogist, Special Publication, no. 5, p. 91–168.

Wiltschko, D. V., and Morse, J. W., 2001, Crystallization pressure versus "crack seal" as a mechanism for banded veins: Geology, v. 29, p. 79–82.

Worden, R. H., Droop, G. T. R., and Champness, P. E., 1991, The reaction antigorite $\Rightarrow$ olivine + talc + H_2O in the Bergell aureole, N. Italy: Mineralogical Magazine, v. 55, p. 367–377.

Wunder, B., and Schreyer, W., 1997, Antigorite: High-pressure stability in the system $MgO-SiO_2-H_2O$ (MSH): Lithos, v. 41, p. 213–227.

Wunder, B., Wirth, R., and Gottschalk, M., 2001, Antigorite: Pressure and temperature dependence of polysomatism and water content: European Journal of Mineralogy, v. 13, p. 485–495.

Yada, K., 1971, Study of microstructure of chrysotile by high-resolution electron microscopy: Acta Crystallographica, v. A27, p. 659–664.

———, 1979, Microstructures of chrysotile and antigorite by high-resolution electron microscopy: Canadian Mineralogist, v. 17, p. 679–692.

Yada, K.. and Iishi, K., 1974, Serpentine minerals hydrothermally synthesized and their microstructures: Journal of Crystal Growth, v. 24/25, p. 627–630.

Yada, K., and Wei, L., 1987, Polygonal microstructures of Povlen chrysotile observed by high-resolution electron microscopy: Paper presented at Euroclay 87, Sevilla, Spain.

Yoder, H. S., 1952, The $MgO-Al_2O_3-SiO_2-H_2O$ system and related metamorphic facies: American Journal of Science, Bowen Volume, p. 569–627.

Zoltai, T., 1981, Amphibole asbestos mineralogy: Reviews in Mineralogy, Vol. 9A, Amphiboles and other hydrous pyriboles–mineralogy, p. 237–279.

Zussman, J., 1954, Investigation of the crystal structure of antigorite: Mineralogical Magazine, v. 30, p. 498–512.